Analysis of the Mechanisms of Mitochondrial NADH Regulation in Cardiac Trabeculae

Rolf Brandes and Donald M. Bers
Department of Physiology, Loyola University, Chicago School of Medicine, 2160 South First Avenue, Maywood, Illinois 60153 USA

ABSTRACT We have previously shown that increased cardiac work initially caused a rapid Ca^{2+}-independent fall of mitochondrial [NADH] ($[NADH]_m$) to a minimum level, and this was followed by a slow Ca^{2+}-dependent recovery toward control level (Brandes and Bers, *Biophys. J.* 71:1024–1035, 1996; Brandes and Bers, *Circ. Res.* 80:82–87, 1997). The purpose of this study is to improve our understanding of the factors that control $[NADH]_m$ during increased work. $[NADH]_m$ was monitored using fluorescence spectroscopy in intact rat trabeculae isolated from the right ventricular wall. Work was increased by increasing sarcomere length, pacing frequency, external $[Ca^{2+}]$, or by decreased temperature. The results were: 1) The initial fall of $[NADH]_m$ during increased pacing frequency depends independently on increased myofilament work and on increased Ca^{2+}-transport ATPase activity. 2) The $[NADH]_m$ recovery process depends on average cytosolic $[Ca^{2+}]$ ($Av[Ca^{2+}]_c$), but not on absolute work level. 3) The initial fall of $[NADH]_m$ and the $[NADH]_m$ recovery are similar whether increased work is associated with low frequency and high Ca^{2+}-transient amplitude or vice versa (at the same myofilament work level and $Av[Ca^{2+}]_c$). 4) The mechanisms associated with the smaller fall and recovery of $[NADH]_m$ at 37°C versus 27°C, may be explained by lowered $Av[Ca^{2+}]_c$ and myofilament work. The NADH control mechanisms that operate at lower temperature are thus qualitatively similar at more physiological temperatures.

DEFINITIONS AND ABBREVIATIONS

SL	=	Sarcomere length
SR	=	Sarcoplasmic reticulum
$[Ca^{2+}]_c$	=	Cytosolic $[Ca^{2+}]$
$[Ca^{2+}]_o$	=	Extracellular $[Ca^{2+}]$
$[Ca^{2+}]_m$	=	Mitochondrial $[Ca^{2+}]$. Depends on $Av[Ca^{2+}]_c$.
$Av[Ca^{2+}]_c$	=	Time-averaged $[Ca^{2+}]_c$. Depends on pacing frequency and Ca^{2+}-transient amplitude (and relaxation rate).
F_{Av}	=	Time-averaged developed force. Depends on $Av[Ca^{2+}]_c$ and SL.
F^0_{Av}	=	Time-averaged developed force for reference protocol (see Table 1, Protocol P0).
W	=	Total (rate of) work performed (= $W_{Force} + W_{Trsp} + W_{other}$).
W_{Force}	=	Work performed by the myofilaments resulting in ATP hydrolysis. Depends on F_{Av}.
W_{Trsp}	=	Work performed by Ca^{2+}-transport resulting in ATP hydrolysis. Depends on $Av[Ca^{2+}]_c$.
W_{other}	=	Work performed by other processes.
NADH	=	Semicalibrated $[NADH]_m$ from Nratio (see Eq. 2) or nicotineamid adenine dinucleotide (reduced form).
$[NADH]_m$	=	Mitochondrial [NADH]
NADH MIN	=	Minimum level of NADH following increased work. Depends independently on increased W_{Force} and W_{Trsp}.
NADH REC	=	Amount of NADH recovery following prolonged work. Depends on $[Ca^{2+}]_m$ (which depends on $Av[Ca^{2+}]_c$).
NADH MAX	=	Maximum level of NADH following reduced work. Depends on $[Ca^{2+}]_m$ (which depends on $Av[Ca^{2+}]_c$) before reducing work.
P0–*n*	=	Going from Protocol P*n* (n = 1–6) to Protocol P0 (Reference protocol) causes changes in the variables controlling NADH and, consequently, in NADH MIN, NADH REC, and NADH MAX.

INTRODUCTION

The mechanisms of the regulation of oxidative phosphorylation with increased work loads are poorly understood. It is, however, clear that $[NADH]_m$ plays a central role as a regulatory signal (Balaban, 1990; From et al., 1990; Hansford, 1994) and as an indicator of the mitochondrial protonmotive gradient. Indeed, recent proposed mechanisms have implicated NADH as a regulator of the oxidative phosphorylation rate where $[NADH]_m$, in turn, is controlled by increased $[Ca^{2+}]_m$ (Hansford, 1991). Our previous results partially agree with this idea, but have shown that the regulation is more complex and involves at least two control mechanisms. When the work level was abruptly increased, there was an initial drop of $[NADH]_m$, which was followed by a slow recovery, and an overshoot after the work level

Received for publication 31 August 1998 and in final form 26 May 1999.
Address reprint requests to Rolf Brandes, Department of Physiology, Loyola University–Chicago, School of Medicine, 2160 South First Avenue, Maywood, IL 60153. Tel.: 708-216-6305; Fax: 708-216-6308; E-mail: rbrande@luc.edu.

0006-3495/99/09/1666/17 $2.00

was returned to control (Brandes and Bers, 1996a; Brandes and Bers, 1997).

Figure 1 shows our current hypothetical mechanism of $[NADH]_m$ regulation. When work is abruptly increased by increased pacing frequency (e.g., from 0.25 to 2 Hz) or by increased Ca^{2+}-transient amplitude (e.g., by increased $[Ca^{2+}]_o$), $Av[Ca^{2+}]_c$, and F_{Av} is expected to instantaneously increase. Initially, the sudden increase in work load and ATP hydrolysis rate may result in increased [ADP] (or $[P_i]$), which may stimulate the oxidative phosphorylation rate and, thereby, a fall of $[NADH]_m$ (to NADH MIN). In this study, we will discuss two separate types of work causing ATP hydrolysis: work depending on F_{Av} (myofilament force generation; W_{Force}), and work depending on $Av[Ca^{2+}]_c$ (e.g., sarcoplasmic reticulum Ca^{2+}-transport; W_{Trsp}).

An increase in $Av[Ca^{2+}]_c$ is also expected to independently cause a slow (time-constant ~30 s) increase in $[Ca^{2+}]_m$, activating pyruvate dehydrogenase and/or tricarboxylic acid cycle dehydrogenases (Crompton, 1990; McCormack et al., 1990; Hansford, 1991) and thereby increases the NADH production rate. This increased production rate causes $[NADH]_m$ to recover (by NADH REC) and reach a new steady-state level close to the original control level. When the pacing frequency (and therefore adenosine triphosphate (ATP) hydrolysis rate) is lowered back to control work, the time-lag of $[Ca^{2+}]_m$ removal causes $[NADH]_m$ to overshoot (to NADH MAX). Note that the NADH fall and recovery may be less apparent under conditions where work is more gradually increased, and the fall would be prevented by coincidental recovery.

Our previous results were consistent with this hypothesis. When work was increased using a protocol that increased $Av[Ca^{2+}]_c$ (e.g., increased pacing frequency or $[Ca^{2+}]_o$) the $[NADH]_m$ decline was followed by recovery and overshoot (Brandes and Bers, 1997). In contrast, when work was increased using a protocol that was not expected to significantly increase $Av[Ca^{2+}]_c$ (by increasing sarcomere length), $[NADH]_m$ still declined, but there was no recovery or overshoot (Brandes and Bers, 1997). In both types of protocol, increased work caused a fall of $[NADH]_m$, although the type of work differed; increased frequency (or $[Ca^{2+}]_o$) is expected to cause increased W_{Force} and W_{Trsp}, whereas increased sarcomere length is expected to only cause increased W_{Force}. The first goal of this study is thus to evaluate the relative importance of W_{Force} versus W_{Trsp} in stimulating oxidative phosphorylation and thereby cause the initial fall of $[NADH]_m$.

Previous studies have shown that not only increased Ca^{2+}, but also increased ADP/ATP ratio may stimulate the TCA cycle (Crompton, 1990) and thereby possibly cause $[NADH]_m$ recovery. Although we did not observe any (slow) recovery when work was increased in the absence of increased $Av[Ca^{2+}]_c$, it is possible that increased ADP/ATP, with increased W_{Force}, alters the Ca^{2+}-sensitivity ($K_{0.5}$) of the mitochondrial dehydrogenases (McCormack et al., 1990). The second goal of this study is thus to determine whether the Ca^{2+}-dependent NADH recovery was influenced by myofilament work level (W_{Force}).

Increased W_{Force} is expected to be directly related to increased F_{Av}, regardless of how F_{Av} is increased, e.g., by increased SL, frequency, or Ca^{2+}-transient amplitude (using increased $[Ca^{2+}]_o$). In contrast, at the same F_{Av}, the increase in W_{Trsp}, and consequently the fall of $[NADH]_m$, may differ when work is increased by increased frequency versus increased Ca^{2+}-transient amplitude because the SR Ca^{2+}

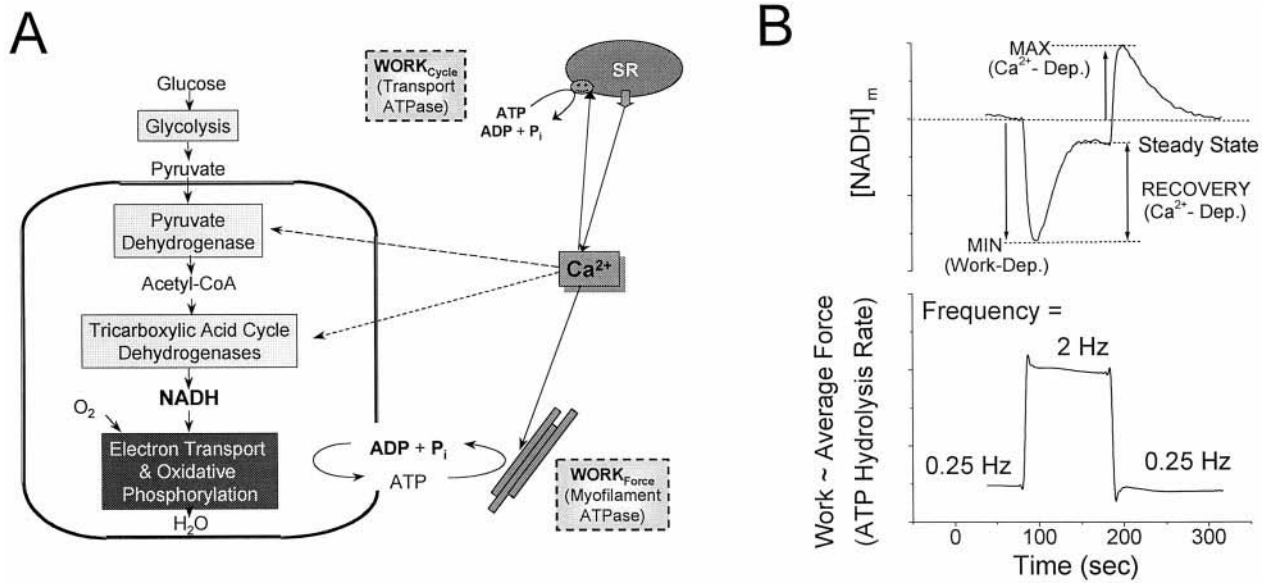

FIGURE 1 Hypothetical mechanism for control of $[NADH]_m$ (see text). *A*. Schematic diagram of the role of Ca^{2+} in stimulating myofilament and sarcoplasmic reticulum ATPase in addition to increasing the NADH production rate via activation of mitochondrial dehydrogenases. *B*. Altered pacing frequency (from 0.25 to 2 to 0.25 Hz) causes a work-jump (transiently increased ATP hydrolysis rate) and dynamic regulation of $[NADH]_m$ as defined by NADH MIN, NADH REC, NADH steady state, and NADH MAX.

ATPase activity may differ under these two conditions. Similarly, $[Ca^{2+}]_m$-uptake and consequently the $[NADH]_m$ recovery, may differ at the same $Av[Ca^{2+}]_c$, depending on whether the uptake process is differentially sensitive to frequency versus Ca^{2+}-transient amplitude. The third goal is therefore to determine if W_{Trsp} and mitochondrial Ca^{2+}-uptake depends on pacing frequency versus Ca^{2+}-transient amplitude as assessed from the effects on $[NADH]_m$ fall and recovery.

We have previously demonstrated that the characteristic changes in $[NADH]_m$ depicted in Fig. 1 occur at both 24°C and 37°C (Brandes and Bers, 1997). However, higher pacing frequencies were needed to observe similar extents of NADH decline and recovery at 37°C as at 24°C. This difference could be due to lower $[Ca^{2+}]_c$ at 37°C, causing lower $Av[Ca^{2+}]_c$ and consequently lower work (Puglisi et al., 1996). Our fourth goal is thus to evaluate whether altered NADH regulation at higher temperatures can be mimicked by lowering $[Ca^{2+}]_o$.

MATERIALS AND METHODS

Trabeculae preparation and solutions

Thin band-shaped trabeculae (~200 × 500 μm) were isolated from rat right ventricles as described elsewhere (Brandes and Bers, 1996a). Briefly, brown male LBN-F1 rats (~350–500 g) were deeply anesthetized and anticoagulated by injecting 65 mg pentobarbital and 1000 U heparin i.p. The hearts were excised and then perfused retrograde before removing the trabeculae. The perfusion solution contained (in mM): NaCl (108), KCl (21), $MgCl_2$ (1.2), $CaCl_2$ (0.5), $NaHCO_3$ (24), Glucose (4), sodium pyruvate (10), insulin (20 units/L) and was equilibrated with a 95% O_2, 5% CO_2 gas mixture to produce pH = 7.40 (adjusted at the appropriate temperature). Note that, as in our previous studies (Brandes and Bers, 1996a; Brandes and Bers, 1997), we have used high concentrations of pyruvate to strongly activate pyruvate dehydrogenase, rendering it potentially less sensitive to activation/phosphorylation by Ca^{2+} (Kobayashi and Neely, 1983), and thereby simplifying interpretation of the data.

After dissection, the muscle was mounted in a muscle chamber, paced at 0.25 Hz and superfused at 10–15 mL/min with the solution described above, except that 6 mM KCl, instead of 21 mM, was used. This solution was used for all experiments except for the $[Ca^{2+}]_o$, which depended on protocol (see below). Muscle force was measured during isometric contractions, and SL was varied by adjusting muscle stretch. Sarcomere length was assessed from laser light (Uniphase 102-4) diffraction patterns, created by transmitting the light through the muscle (Backx and Ter Keurs, 1993).

$[NADH]_m$ measurements and calibration

$[NADH]_m$ was assessed using methods described previously (Brandes and Bers, 1996a). Briefly, the trabeculae were excited by light at 350 nm, and fluorescence detected at 385 and 456 nm. The use of these tissue light isosbestic wavelengths accounts for possible changes in tissue light absorbance, e.g., due to hypoxia (Brandes et al., 1994). However, as we have demonstrated, the trabeculae were not hypoxic at higher pacing rates (Brandes and Bers, 1996a). The fluorescence signal at 456 nm (N456) is predominantly arising from mitochondrial NADH (Nuutinen, 1984; Eng et al., 1989) and motion artifacts. In contrast, the reference signal at 385 nm (due to autofluorescence and possibly a small component of back-scattered light; N385) is mainly sensitive to motion artifacts (Brandes and Bers, 1996a). We therefore used our previously developed method to eliminate motion artifacts from the NADH fluorescence signal at 456 nm by dividing it with the reference signal (Brandes and Bers, 1996a), thus obtaining a fluorescence ratio (Nratio),

$$\text{Nratio} = \frac{\text{N456}}{\text{N385}} \tag{1}$$

Because N385 and N456 gradually decreased during the experimental protocols, and at different rates (Ashruf et al., 1995; Brandes and Bers, 1996b), Nratio was normalized relative to its value at a pacing frequency of 0.25 Hz (control value). Occasionally, Nratio slowly changed during the course of a protocol and, in this case, the whole trace was mathematically baseline corrected by normalizing consecutive Nratios at 0.25 Hz (e.g., see Fig. 2 *A*). The ratio was calibrated by assuming a minimum (maximally oxidized) value of $[NADH]_m$ corresponding to 0.49·Nratio (at 1 Hz) (Brandes and Bers, 1996a). The relative $[NADH]_m$ was thus calculated from the measured Nratio to obtain semicalibrated NADH according to

$$\text{NADH} = \frac{\text{Nratio} - 0.49 \cdot \text{Nratio(1 Hz)}}{\text{Nratio(0.25 Hz)} - 0.49 \cdot \text{Nratio(1 Hz)}} \tag{2}$$

Note that, because Nratio(0 Hz) ~ Nratio(0.25 Hz), calibrated NADH would be similar regardless of whether 0 or 0.25 Hz were used as baseline condition. This calibration procedure causes the changes in NADH to be up to twice as large as the changes in Nratio (e.g., a 10% change in Nratio would result in a 15–20% change in the calibrated NADH). Changes in NADH will be expressed in absolute fractional or percentage units, where NADH at control is unity (1) or 100% (per Eq. 2).

Assessment of myofilament-related ATP hydrolysis rate and data analysis

Isometric muscle force was measured using a force transducer as described elsewhere (Brandes and Bers, 1996a), from which developed force (difference between active and resting force) was calculated. F_{Av} was used as an index of ATP hydrolysis rate related to force generation (Brandes and Bers, 1996a) and was normalized to muscle cross-sectional area. This indirect and simplified measure assumes that the ATP hydrolysis rate is related to active force during the whole (isometric) contraction cycle (Cooper, 1979). A 0.2-Hz low-pass filter was applied to the developed force signal to obtain F_{Av} by using software digital filtering (Origin, MicroCal Software Incorporated, Northampton, MA). Because F_{Av} was not constant following increased frequency, NADH and F_{Av} were always compared at the same point in time (e.g., at NADH MIN or NADH at steady-state).

Improved signal-to-noise ratio of the calculated NADH signal was also obtained by digital low-pass filtering. Results were reported as means ± standard error. Statistical analysis was performed using Student's *t*-test, paired where applicable, and differences were considered significant when $p < 0.05$. To determine the minimum number of parameters needed to calculate the three-dimensional (3D) surface used for data interpolation (see Results) an *F* test was performed; Going from a model with six to five parameters increased the degrees of freedom and sum-of-squares. Only if the relative increase in the sum-of-squares was significantly larger than the relative increase in the degrees of freedom (based on the *F* test), would the more complicated six-parameter model be deemed more appropriate.

PROTOCOLS AND INTERPRETATIVE FRAMEWORK

The baseline experiment was to investigate the effect of pacing frequency on $[NADH]_m$ by increasing it from a control of 0.25 Hz to either 0.5, 1, 2, or 3 Hz, and then back to 0.25 Hz. Note that each frequency step would cause a different NADH response and consequently different MIN, REC and MAX. This experiment was then repeated after

changing either SL, $[Ca^{2+}]_o$, or temperature. Thus, the effects of sarcomere length on the frequency–NADH (MIN, REC, and MAX) relationship were investigated by repeating the pacing sequence at various sarcomere lengths from approximately 1.7 to 2.1 μm. Similarly, the effects of $[Ca^{2+}]_o$ or temperature on the frequency–NADH relationship were investigated by repeating the pacing sequence at various $[Ca^{2+}]_o$ (from 0.3 to 2 mM) and temperatures (27°C and 37°C). However, to separate the individual effects of $Av[Ca^{2+}]_c$ W_{Force} and W_{Trsp} on NADH MIN, NADH REC, and NADH MAX, extensive data analysis is needed.

A protocol is defined as a work-jump using a frequency step (from 0.25 Hz to a higher value) at a particular SL, $[Ca^{2+}]_o$, and temperature. Different protocols would produce different values of the variables controlling $[NADH]_m$ ($Av[Ca^{2+}]_c$, W_{Force}, and W_{Trsp}), and therefore result in different NADH MIN, NADH REC, and NADH MAX. By comparing two such protocols, one protocol will have a larger $Av[Ca^{2+}]_c$, W_{Force}, or W_{Trsp} than the other and consequently cause larger or smaller NADH MIN, NADH REC, and NADH MAX.

For example, in a reference protocol SL = 2.1 μm, $[Ca^{2+}]_o$ = 2.0 mM, and frequency 2 Hz (i.e., jump from 0.25 to 2 Hz), whereas, in another protocol, only SL is reduced to 1.9 μm while $[Ca^{2+}]_o$ and frequency are unchanged (2 mM and 0.25 to 2 Hz, respectively). In this case, the reference protocol is expected to produce a larger W_{Force} (because of the longer SL), whereas $Av[Ca^{2+}]_c$ and W_{Trsp} are expected to be similar (since small changes in SL are not expected to cause significant changes in $Av[Ca^{2+}]_c$ and, consequently, also not in W_{Trsp} (Kentish and Wrzosek, 1998)). The larger W_{Force} is expected to cause a larger fall of $[NADH]_m$ (lower NADH MIN), while the similar $Av[Ca^{2+}]_c$ may result in similar NADH REC and NADH-MAX.

In Table 1, we have defined six different protocols where one or two variables (frequency jump, sarcomere length, or $[Ca^{2+}]_o$) are altered relative to a maximal reference protocol (P0). Comparison of each protocol versus this maximal reference protocol are expected to cause the indicated changes in the variables controlling $[NADH]_m$ ($Av[Ca^{2+}]_c$, W_{Force}, and W_{Trsp}). Table 1 also shows the hypothetical (to be tested experimentally) changes in NADH MIN, NADH REC, and NADH MAX given the expected changes in $Av[Ca^{2+}]_c$, W_{Force}, and W_{Trsp}.

TABLE 1 Protocols used to change control variables: W_{Force}, W_{Trsp} and $Av[Ca^{2+}]_c$ alone or in combination. Going from a protocol P*n* to the Reference protocol P0 may cause an increase in control variables and the expected effects on NADH MIN (ΔMIN), NADH REC (ΔREC) and NADH MAX (ΔMAX) are shown symbolically; increased (↑), decreased (↓), or unchanged (=) (see also Results). The numbers in squares correspond to the numbers in squares in Figs. 3 *A* and 5 *A*.

Protocol	Conditions	Main Purpose (Independent Parameters)	ΔControl Variables (P0–P*n*)	ΔMIN (Work Dep.)	ΔREC (Ca^{2+}-Dep.)	ΔMAX (Ca^{2+}-Dep.)	Used in Figures
P0	SL = 2.1 μm Freq. = 2 Hz* $[Ca^{2+}]_o$ = 2 mM (0 in Fig. 3)	Main Maximal Reference (F^0_{Av}, 2 Hz)	—	—	—	—	3, 5A, 4, 7
P1	SL = 2.1 μm **Freq. = 1 Hz*** $[Ca^{2+}]_o$ = 2 mM	Increased W_{Trsp} and W_{Force} (**F^0_{Av}/1.5, 1 Hz**)	↑ W_{Force} ↑ W_{Trsp} ↑ $Av[Ca^{2+}]_c$	↓ ↓	↑	↑	2B, 6B, 4B, 7B
P2	SL = 2.1 μm **Freq. ~ 0.7 Hz*** $[Ca^{2+}]_o$ = 2 mM	Increased W_{Trsp} and W_{Force} (**F^0_{Av}/2, ~0.7 Hz**)	↑ W_{Force} ↑ W_{Trsp} ↑ $Av[Ca^{2+}]_c$	↓ ↓	↑	↑	2C, 6C, 4B, 7B
P3	**SL < 2.1 μm**# Freq. = 2 Hz* $[Ca^{2+}]_o$ = 2 mM (3 in Fig. 3)	Increased W_{Force} only (**F^0_{Av}/2**, 2 Hz)	↑ W_{Force} = W_{Trsp} = $Av[Ca^{2+}]_c$	↓	=	=	3, 5A, 4
P4	**SL > 2.1 μm**# **Freq. = 1 Hz*** $[Ca^{2+}]_o$ = 2 mM (4 in Fig. 3)	Increased W_{Trsp} only (F^0_{Av}, **1 Hz**)	= W_{Force} ↑ W_{Trsp} ↑ $Av[Ca^{2+}]_c$	↓	↑	↑	3, 5A, 4
P5	SL = 2.1 μm Freq. = 2 Hz* **$[Ca^{2+}]_o$ < 2 mM**#	Increased W_{Trsp} and W_{Force} (**F^0_{Av}/2**, 2 Hz)	↑ W_{Force} ↑ W_{Trsp} ↑ $Av[Ca^{2+}]_c$	↓ ↓	↑	↑	7
P6	SL = 2.1 μm **Freq. = 1 Hz*** **$[Ca^{2+}]_o$ > 2 mM**#	Compare Freq. vs. Ca^{2+}-Ampl (F^0_{Av}, **1 Hz**)	= W_{Force} = W_{Trsp} = $Av[Ca^{2+}]_c$	=	=	=	7

*In all protocols, a work-jump was obtained by increasing the pacing frequency from control (0.25 Hz) to a higher value (e.g., ~0.7, 1, or 2 Hz).
#Interpolated or extrapolated values from surface fit (e.g., Fig. 3 *A*). Parameters in bold typeface denote changes in conditions relative to the maximal Reference Protocol (P0).

Protocols at $T = 27°C$ (see Table 1)

Protocol 0. A common maximal reference protocol P0 was first selected. Here, the pacing frequency was increased by jumping to 2 Hz (from 0.25 Hz baseline frequency) at $[Ca^{2+}]_o = 2$ mM and optimum sarcomere length (~2.1 μm) resulting in maximum $\boldsymbol{F}^0_{Av}$.

Protocol 1. P1 is used to evaluate the effects of altered frequency and, consequently, $\boldsymbol{W}_{Trsp}$, $\boldsymbol{W}_{Force}$, and $Av[Ca^{2+}]_c$ on $[NADH]_m$. To do this, the pacing frequency is increased from 0.25 to 1 Hz (versus 2 Hz for P0). A frequency jump to 2 Hz (P0) versus 1 Hz (P1), is expected to cause larger $\boldsymbol{W}_{Trsp}$ and $\boldsymbol{W}_{Force}$, and, consequently, lower NADH MIN, whereas the increased $Av[Ca^{2+}]_c$ is expected to cause larger NADH REC and NADH MAX.

Protocol 2. P2 is similar to P1, but, in this case, the pacing frequency is increased from 0.25 to only ~0.7 Hz (see Results) such that the resulting $\boldsymbol{F}_{Av}$ is half of the Reference value ($\boldsymbol{F}^0_{Av}/2$ versus $\boldsymbol{F}^0_{Av}$ for a jump to 2 Hz). Because P0 is again expected to cause larger $\boldsymbol{W}_{Trsp}$, $\boldsymbol{W}_{Force}$, and $Av[Ca^{2+}]_c$ than this protocol, NADH MIN is expected to be lower, and NADH REC and NADH MAX are expected to be larger.

Protocol 3. P3 is used to evaluate the effects of increased $\boldsymbol{W}_{Force}$ at constant $\boldsymbol{W}_{Trsp}$ (and $Av[Ca^{2+}]_c$) on $[NADH]_m$. To do this, the SL is shorter* so that the same frequency jump as in P0 produces $\boldsymbol{F}^0_{Av}/2$ (i.e., again half of Reference $\boldsymbol{F}^0_{Av}$). P0 is expected to cause larger $\boldsymbol{W}_{Force}$ but similar $\boldsymbol{W}_{Trsp}$ and $Av[Ca^{2+}]$ (because the same frequency and $[Ca^{2+}]_o$ are used in both protocols). Consequently, this comparison isolates elevated $\boldsymbol{W}_{Force}$, which is expected to cause lower NADH MIN, whereas the similar $Av[Ca^{2+}]$ is expected to cause unchanged NADH REC and NADH MAX.

Protocol 4. P4 is used to evaluate the effects of increased $\boldsymbol{W}_{Trsp}$ (and $Av[Ca^{2+}]_c$) at constant $\boldsymbol{W}_{Force}$ on $[NADH]_m$. To do this, the frequency jump is only to 1 Hz, but at a longer SL so that $\boldsymbol{F}_{Av}$ and, consequently, $\boldsymbol{W}_{Force}$ is the same as that at 2 Hz, and SL = 2.1 μm (Reference). Thus, the Reference is expected to have only higher $\boldsymbol{W}_{Trsp}$, resulting in $\boldsymbol{W}_{Trsp}$-dependent lowering of NADH MIN, whereas the larger $Av[Ca^{2+}]_c$ is expected to cause larger NADH REC and NADH MAX.

Protocol 5. P5 is used in conjunction with P2 to differentiate the effects of altered Ca^{2+}-amplitude versus altered frequency on $\boldsymbol{W}_{Trsp}$ and $[Ca^{2+}]_m$-uptake (at constant $\boldsymbol{W}_{Force}$ and $Av[Ca^{2+}]_c$). In P2, $\boldsymbol{F}^0_{Av}/2$ was obtained by a frequency jump to ~0.7 Hz at $[Ca^{2+}]_o = 2$ mM. For comparison here, $\boldsymbol{F}^0_{Av}/2$ is instead obtained by using a frequency jump to 2 Hz, and using lower $[Ca^{2+}]_o$. If these equivalent changes in $\boldsymbol{F}_{Av}$ (versus the Reference) cause equivalent changes in NADH MIN, NADH REC, and NADH MAX, then $\boldsymbol{W}_{Trsp}$ and $[Ca^{2+}[_m$-uptake would be similar regardless of how $\boldsymbol{W}_{Trsp}$ and $Av[Ca^{2+}]_c$ was increased (increased $[Ca^{2+}]_o$ versus frequency).

Protocol 6. P6 is used as an alternative way of differentiating the effects of altered Ca^{2+}-amplitude versus altered frequency on $\boldsymbol{W}_{Trsp}$ and $[Ca^{2+}]_m$-uptake. To do this, the frequency jump here is to only 1 Hz but at a higher $[Ca^{2+}]_o$ so that $\boldsymbol{F}_{Av}$, and consequently $\boldsymbol{W}_{Force}$, is similar to that at 2 Hz and $[Ca^{2+}]_o = 2.0$ mM (Reference, $\boldsymbol{F}_{Av} = \boldsymbol{F}^0_{Av}$). If NADH MIN, NADH REC, and NADH MAX are similar as with P0, then $\boldsymbol{W}_{Trsp}$ and $[Ca^{2+}]_m$-uptake would be similar regardless of how $\boldsymbol{W}_{Trsp}$ and $Av[Ca^{2+}]_c$ was increased (increased $[Ca^{2+}]_o$ versus frequency).

To compare two protocols, e.g., P0 versus P3, the shorthand notation P0–3 will be used to indicate differences both in the controlling variables (which are equal or higher for the P0) and in the resulting NADH MIN, NADH REC, and NADH MAX (i.e., ΔMIN, ΔREC, and ΔMAX).

RESULTS

Effects of sarcomere length (and frequency) on $[NADH]_m$ regulation

Increasing SL is expected to increase F_{Av} and, consequently, W_{Force}, but not significantly affect $Av[Ca^{2+}]_c$ and, consequently, not W_{Trsp}. Figure 2 *A* shows a representative example of the $[NADH]_m$ response to increasing frequency at SL = 2.1 and 1.9 μm. As expected, F_{Av} increases with increasing frequency and is larger at the longer SL. However, because of a negative force–frequency relationship and a faster force relaxation rate at higher frequencies (Maier et al., 1998), doubling the frequency did not cause a doubling of F_{Av}. For example, at SL = 2.1 μm, doubling the frequency from 1 to 2 Hz, caused F_{Av} to only increase by a factor of 1.53 ± 0.032 (at a time corresponding to NADH MIN; $N = 6$). Conversely, to double F_{Av}, the frequency had to be increased from ~0.7 to 2 Hz. The changes in $[NADH]_m$, in response to changes in frequency, are qualitatively, but not quantitatively, similar at both SLs.

$[NADH]_m$ *versus frequency.* To quantify the relationship between $[NADH]_m$ and frequency, the NADH MIN, NADH REC, and NADH MAX (see Fig. 1 *B* for definitions) were obtained from the data in Fig. 2 *A* at SL = 2.1 and 1.9 μm. The example in Fig. 2 *B* shows that, at both SLs, increased frequency caused a progressive decline of NADH MIN, but this decline was more severe at the longer SL. In contrast, NADH REC and NADH MAX were independent of SL and both increased with frequency. Note that increasing frequency, at a constant SL, corresponds to increased W_{Force}, W_{Trsp}, and $Av[Ca^{2+}]_c$ (Brandes and Bers, 1997), whereas increased SL at a constant frequency (e.g., 3 Hz) only corresponds to increased W_{Force}. The lower NADH MIN at the longer SL (e.g., at 3 Hz) may therefore be solely due to higher W_{Force}. Conversely, the unchanged NADH REC and NADH MAX (when increasing SL) may indicate that these parameters are independent of W_{Force}, and solely dependent

* Instead of actually adjusting sarcomere length, $[Ca^{2+}]_o$, or temperature to obtain constant F_{Av} and W_{Force} as described above, fixed values of these variables were used instead. The data were then interpolated or extrapolated on a 3D surface to obtain constant F_{Av} and W_{Force} (see Results and Figs. 3 *A* and 5 *A*).

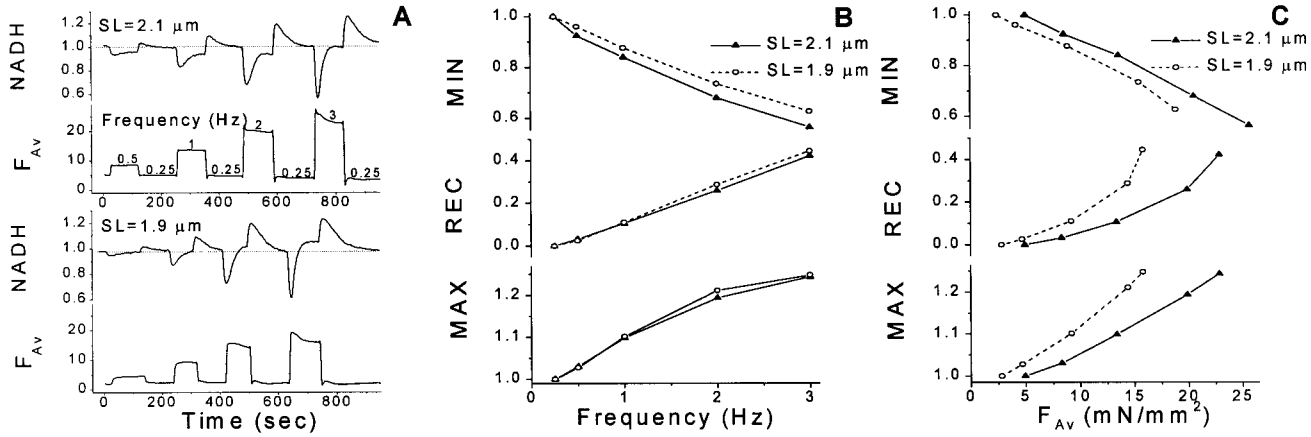

FIGURE 2 A typical example of the effects of increased pacing frequency (increased work and Av$[Ca^{2+}]_c$) and increased sarcomere length (increased work at constant Av$[Ca^{2+}]_c$) on $[NADH]_m$. *A*. Time-traces of average force (F_{Av}; mN/mm^2) and NADH (relative to 0.25 Hz) as frequency was increased from control of 0.25 Hz to 0.5, 1, 2, or 3 Hz, and then back to 0.25 Hz at SL = 1.9 or 2.1 μm. *B*. NADH MIN, NADH REC, and NADH MAX as a function of pacing frequency and SL. *C*. NADH MIN, NADH REC, and NADH MAX as a function of F_{Av} and SL. F_{Av} was obtained at each pacing frequency (0.25, 0.5, 1, 2, and 3 Hz) from Fig. 2 *A*.

on Av$[Ca^{2+}]_c$. A simple way of quantifying the sensitivity of NADH to increased frequency is to calculate the change in NADH for a 1-Hz change or doubling in frequency (Table 1, P0 versus P1 or simply P0–1). When the frequency was increased to 2 rather than to 1 Hz at SL = 2.1 μm and $[Ca^{2+}]_o$ = 2 mM, NADH MIN was lower by 0.142 ± 0.0135 units (14.2%), NADH REC was larger by 0.101 ± 0.0115 units (10.1%) and NADH MAX was larger by 0.0724 ± 0.0163 units (7.24%) (N = 6).

$[NADH]_m$ *versus* F_{Av}. Figure 2 *C* shows the same example data graphed as a function of F_{Av}. At any given F_{Av}, MIN is higher at SL = 2.1 than at 1.9 μm. Thus, there still seems to be a W_{Force}-independent component of MIN when going from SL = 2.1 to 1.9 μm, where increased frequency or W_{Trsp} seems to lower MIN. That is, the corresponding F_{Av} at SL = 1.9 μm occurs at a higher frequency. Of course, for REC and MAX, that seemed to depend only on Av$[Ca^{2+}]_c$ (Fig. 2 *B*), these parameters were higher at SL = 1.9 μm and the higher frequency required to produce the same F_{Av} as at SL = 2.1 μm.

To determine the effects of doubling F_{Av} (by increased frequency at SL = 2.1 μm) on NADH MIN, NADH MAX, and NADH REC (Table 1, P0–2), the F_{Av} and NADH values for the Reference conditions ($[Ca^{2+}]_o$ = 2 mM, frequency = 2 Hz, and SL ~ 2.1 μm to obtain max F_{Av} = F^0_{Av}) was first determined. The data in Fig. 2 *C* were then fit to second degree polynomials, and the NADH values at $F^0_{Av}/2$ were found by interpolation. From this analysis, it was found that, when $F^0_{Av}/2$ was doubled (corresponding to increased pacing frequency from ~0.7 to 2 Hz), NADH MIN was lower by 20.4 ± 2.1%, NADH REC was higher by 15.8 ± 1.8% and NADH MAX was higher by 12.1 ± 1.0% (N = 6).

A fundamental limitation of the analysis above is that increased frequency increases both W_{Force}, and W_{Trsp}, (and Av$[Ca^{2+}]_c$). For the aims of the present study, we need to separate these influences on NADH MIN, NADH REC, and NADH MAX.

Comparing the Effects of W_{Force} versus W_{Trsp} on NADH MIN

To separate the individual effects of W_{Force} and W_{Trsp} on NADH MIN (our first goal), it would be advantageous to vary W_{Trsp} while holding W_{Force} constant and vice versa. For example, the increase in W_{Force}, produced by increased frequency, can be compensated for by reducing SL such that F_{Av} and, therefore, presumably, W_{Force} are constant. However this is very difficult to achieve experimentally. A simpler, alternative approach is to extend the analysis of the data from the SL/frequency experiments above (Fig. 2) to allow interpolation to the ideal data points. Figure 3 *A* shows a representative 3D analysis of NADH MIN (z axis) as a function of frequency (x axis) at three different sarcomere lengths (using a different muscle than that in Fig. 2). Also shown is the calculated F_{Av} (y axis), which results from the given combination of frequency and SL. The spheres are the measured NADH MIN data points, which depend on SL and pacing frequency (and consequently on F_{Av}). The framed numbers in the graph correspond to the protocols in Table 1, and will be further discussed below. The wire-frame surface was calculated from a semi-empirical relationship of NADH MIN versus frequency and F_{Av} given by

$$\text{NADH MIN} = \alpha + \beta \cdot \text{Freq} + \gamma \cdot \text{Freq}^2 + \delta \cdot F_{Av} + \epsilon \cdot F^2_{Av} + \phi \cdot \text{Freq} \cdot F_{Av}, \quad (3)$$

where α, β, γ, δ, ϵ, and ϕ are constants obtained from a multiple regression fit of the NADH data. Note that there is no physical basis for this equation, its only purpose is to obtain a surface from which one can interpolate data points

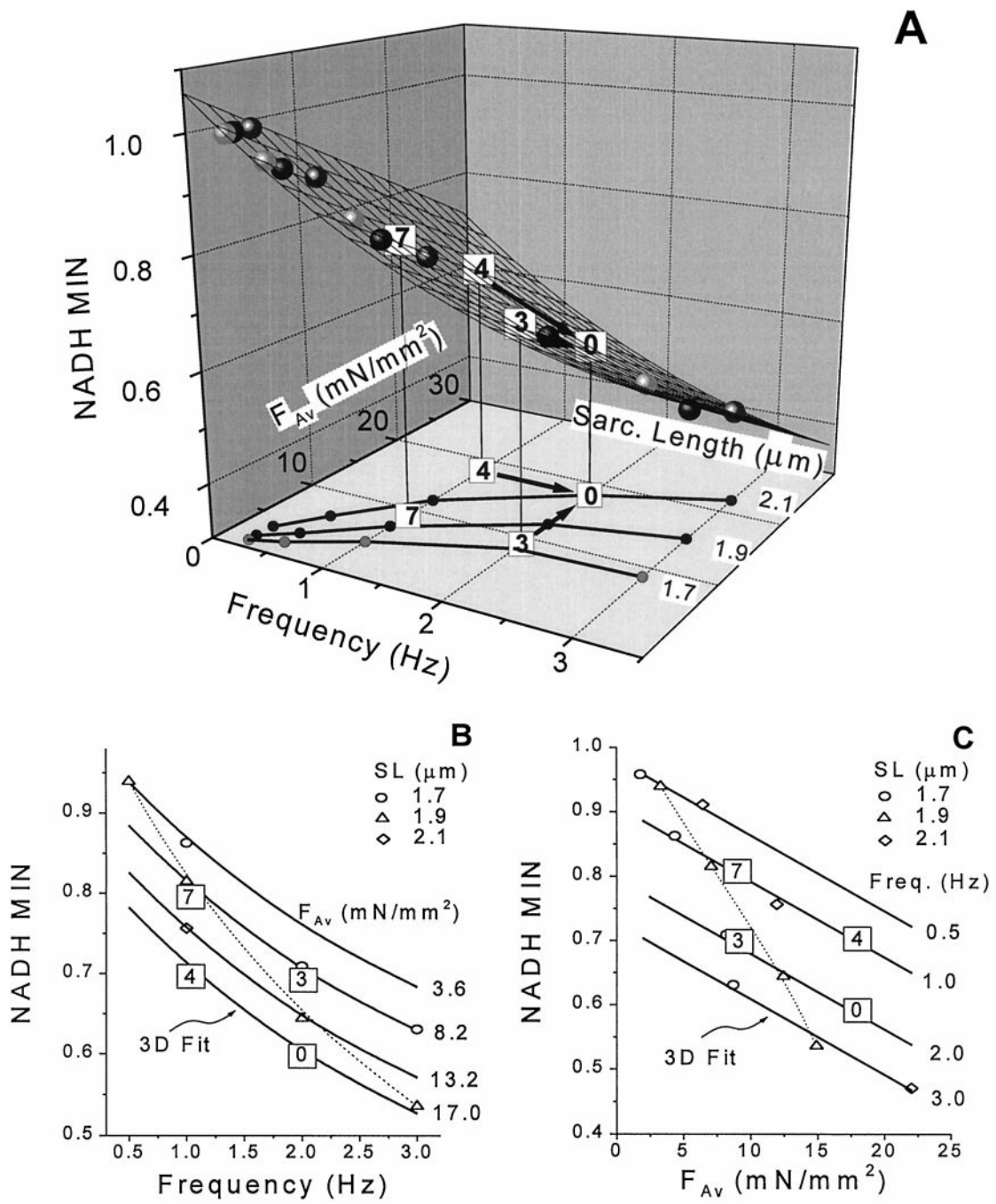

FIGURE 3 A typical example of the relationship between NADH MIN (z axis) versus pacing frequency (x axis) and calculated F_{Av} (y axis). *A*. The spheres are the NADH MIN data points, obtained at the indicated frequency and SL (producing the calculated F_{Av} on the y axis). The wire-frame surface was calculated using a multiple linear regression fit (see Eq. 3). The numbers in squares (at Reference and comparison points) are calculated NADH MIN values at various frequencies and F_{Av}s (see Table 1). *B*. NADH MIN versus frequency along lines of constant F_{Av}, calculated from the fitted surface parameters. *C*. NADH MIN versus F_{Av} along lines of constant frequency (Freq.), calculated from the fitted surface parameters. Relevant data points at various sarcomere lengths and the Reference and comparison points are also shown in *B* and *C*. The dotted lines *B* and *C* were obtained by connecting the points for SL = 1.9 μm (for comparison with Fig. 2, *B* and *C*).

not directly measured experimentally. To simplify, the curve fitting was first performed while excluding the interdependent or interactive "$\phi \cdot \text{Freq} \cdot F_{Av}$" term (the justification for this will be explored below).

Figure 3 *A* also shows the projection of the data spheres on the x–y plane (Frequency–F_{Av} plane), demonstrating the relationship between frequency and F_{Av} at the different sarcomere lengths used; 1.7, 1.9, and 2.1 μm. Increasing frequency at a fixed SL caused increasing F_{Av}, and the increase in F_{Av} was more pronounced at longer SLs.

Figure 3 *B* shows the projection of (some of) the data spheres in Fig. 3 *A* on the x–z plane, demonstrating the

relationship between frequency and NADH MIN at the different sarcomere lengths used, similar to Fig. 2 *B*. However, in Fig. 2 *B*, the data points were connected at fixed SLs (*dotted line* in Fig. 3 *B* for SL 1.9 μm), whereas, in Fig. 3 *B*, the data points are connected by solid lines of constant F_{Av} (NADH MIN lines calculated using the parameters from the fitted surface). The advantage of the curves in Fig. 3 *B* is that they describe the pure influence of frequency by W_{Trsp} on MIN, independent of W_{Force}. For all F_{Av} curves shown, increased frequency or W_{Trsp} by itself (without increased F_{Av} or W_{Force}), is sufficient to stimulate oxidative phosphorylation and thereby cause a fall of $[NADH]_m$ (lower NADH MIN).

Figure 3 *C* shows the projection of the data spheres in Fig. 3 *A* on the *y–z* plane, demonstrating the relationship between F_{Av} and NADH MIN at the different sarcomere lengths used, similar to Fig. 2 *C*. However, in Fig. 2 *C*, the data points were connected at fixed SLs (*dotted line* in Fig. 3 *C* for SL 1.9 μm), whereas, in Fig. 3 *C*, the data points are connected by solid lines of constant frequency (NADH MIN lines calculated using the parameters from the fitted surface). Figure 3 *C* demonstrates that increased W_{Force} by itself (without increased W_{Trsp} due to increased frequency) is sufficient to stimulate oxidative phosphorylation and cause a fall of $[NADH]_m$. Figure 3, *B* and *C* combined, suggest that both increased W_{Force} and W_{Trsp} independently contribute to decreased NADH MIN when the pacing frequency is increased.

A simple comparison based on the example in Fig. 3, *B* and *C*, shows that a sixfold increase in frequency (corresponding to increased W_{Trsp}) at constant F_{Av} (and W_{Force}) decreased NADH MIN by ~0.25 units (Fig. 3 *B*). Similarly, a sixfold increase in F_{Av} (corresponding to increased W_{Force}) at constant frequency (and W_{Trsp}) produced a decrease in NADH MIN by ~0.23 units (Fig. 3 *C*). To more quantitatively evaluate the separate influences of W_{Force} and W_{Trsp} on NADH MIN for the entire group of muscles studied, two different methods were used.

In the first method, either F_{Av} (at constant frequency) or frequency (at constant F_{Av}) was doubled (from half of the Reference values), and the effect on NADH MIN was calculated. In the second method, the surface curvature was calculated (using first-order derivatives), and the curvature for NADH MIN along increasing frequency or F_{Av} was determined.

Method 1. As discussed in "Protocols and Interpretative Framework" and Table 1, a main P0 was defined using a frequency = 2 Hz, SL = 2.1 μm, $[Ca^{2+}]_o$ = 2 mM with a resulting $F_{Av} = F^0_{Av}$. By using the fitted parameters from the wire frame surface in Fig. 3 *A*, the NADH MIN values can be calculated at any arbitrary F_{Av} and frequency (Eq. 3). Figure 3 *A* shows the symbol [0] on the frequency-F_{Av} plane to indicate the values of the independent parameters for P0 as well as at the calculated NADH MIN (on the wire frame surface). Similarly, [3] and [4] are shown to indicate the values of the independent parameters and the calculated NADH MIN for the two comparison protocols P3 ($F_{Av} = F^0_{Av}/2$) and P4 (frequency = 1 Hz). Figure 3 *A* also shows [7], corresponding to a secondary reference P7 ($F_{Av} = F^0_{Av}/2$ and frequency = 1 Hz; not shown in Table 1), for the purpose of investigating possible cross-interactions between W_{Force} and W_{Trsp} (see below).

Figure 4 *A* shows pooled data for the main Reference protocol P0 ([0]) and the two comparison protocols, P3 and P4 ([3] & [4]) from six experiments similar to that in Fig. 3 *A*. However, for clarity, Fig. 4 *A* shows the NADH MIN decline (NADH MIN −1) rather than the magnitude (in Fig. 3 *A*). Figure 4 *A* also shows NADH REC and NADH MAX, and these will be discussed in the next section. Increasing the frequency (from 0. 25 Hz) to 2 Hz at $F_{Av} = F^0_{Av}$ (P0; [0]), causes a fall of NADH that may be due to both increased W_{Force} and W_{Trsp}. In contrast, using P3 ([3]) with the same frequency (2 Hz; same W_{Trsp}), but only half the F_{Av} ($F^0_{Av}/2$), or using P4 ([4]) with the same F_{Av} (F^0_{Av}; same W_{Force}), but half the frequency (1 Hz), causes a smaller fall of NADH MIN because either W_{Force} or W_{Trsp} is lower in these two cases.

By calculating the difference in NADH MIN between the reference and comparison protocols (for each individual experiment), the isolated effects of either increased W_{Trsp} or of increased W_{Force} on NADH MIN may be obtained. Thus, the difference P0–3 (Table 1 and Fig. 3 *A* [0]–[3]) reflects the isolated effect of W_{Force} on NADH MIN, whereas the difference P0–4 (Table 1 and Fig. 3 *A* [0]–[4]) reflects the isolated effect of W_{Trsp} on NADH MIN.

Figure 4 *B* shows the pooled results of these calculations, together with the results from the previous analysis of the data in Fig. 2, *B* and *C*, where work was increased by increasing frequency at constant SL and thus increasing both W_{Trsp} and W_{Force} (P0–1 and P0–2). When only W_{Force} was increased (doubling $F^0_{Av}/2$ by increasing SL; P0–3; [0]–[3] in Fig. 3 *A*), NADH MIN was 8.0 ± 2.0% lower, and, when only W_{Trsp} was increased (doubling frequency from 1 to 2 Hz and decreasing SL; P0–4; [0]–[4] in Fig. 3 *A*), it was 9.2 ± 1.1% lower. Thus, the effect of increasing W_{Force} and W_{Trsp} on NADH MIN was comparable (no significant difference), suggesting that, in both cases, the oxidative phosphorylation rate was stimulated similarly.

In a protocol where F_{Av} and frequency were both exactly doubled ([0]–[7] in Fig. 3 *A*), NADH MIN fell by 17.2 ± 1.9% (= 8.0% + 9.2%). This is consistent with the previous analysis of Fig. 2 as shown in Fig. 4 *B*. In one case, when the frequency was doubled (1 to 2 Hz at constant SL), resulting in $F^0_{Av}/1.53$ increasing by a factor of 1.53 (P0–1), NADH MIN was 14.2 ± 1.35% lower. In the other case, when frequency was increased by a factor of 2.9 (~0.7 to 2 Hz at constant SL) so that $F^0_{Av}/2$ doubled (P0–2), NADH MIN was 20.4 ± 2.1% lower. Because F_{Av} was less than doubled in the first case while the frequency was more than doubled in the second, these two cases bracket the fitted value of 17.2%.

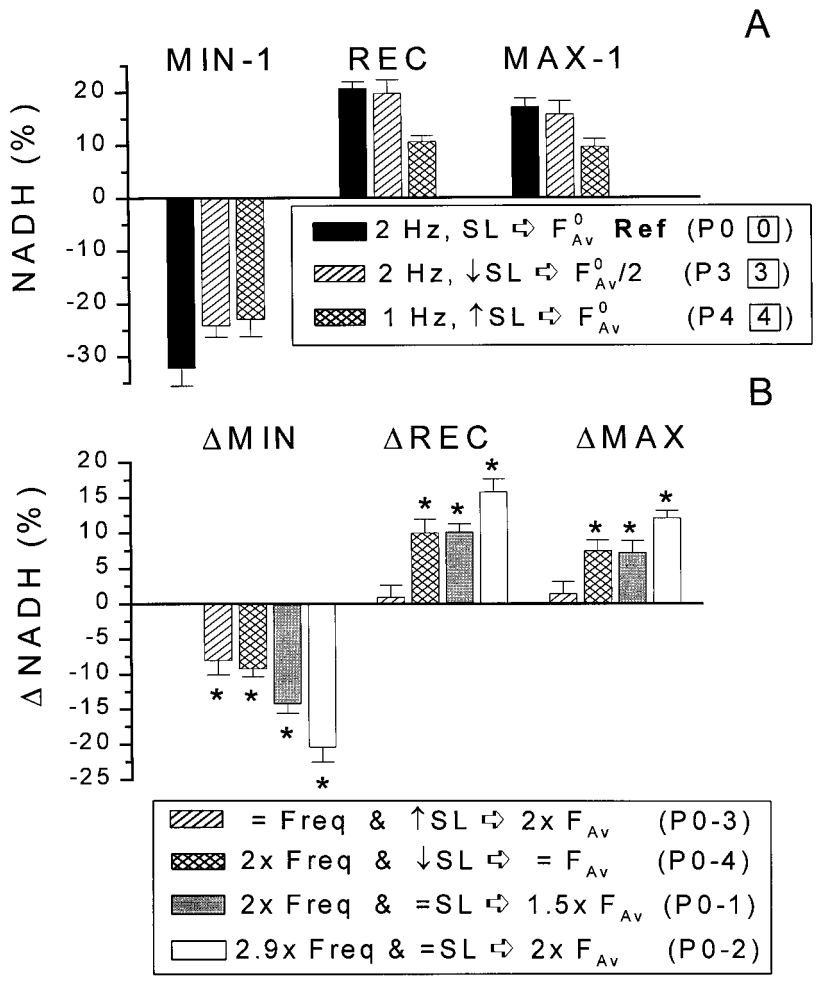

FIGURE 4 Pooled data from fitted wire frame surfaces such as in Figs. 3 *A* and 5 *A* ($N = 6$). *A*. Values for NADH MIN-1, NADH REC, and NADH MAX-1 using Reference protocol P0 (0) and the two comparison protocols P3 and P4 (3 and 4) (see Table 1 and Fig. 3 *A*). *B*. Differences in NADH; ΔMIN, ΔREC, and ΔMAX obtained by subtracting calculated NADH values according to protocols in Table 1; P0–3 (*hatched*; at constant frequency (Freq. = 2 Hz), increase SL to double F_{Av} ($F^0_{Av}/2$ to F^0_{Av}) and P0–4: (*cross-hatched*; double frequency (1 to 2 Hz) and decrease SL to obtain constant F_{Av} (F^0_{Av}). Also shown are the changes calculated from Fig. 2 according to P0–1 (*gray*); double frequency (1 to 2 Hz at constant SL) to increase F_{Av} 1.5 times ($F^0_{Av}/1.5$ to F^0_{Av}) and P0–2 (*white*); increase frequency 2.9 times (~0.7 to 2 Hz at constant SL) to double F_{Av} ($F^0_{Av}/2$ to F^0_{Av}). The * indicates that a difference is significantly larger than zero. Table 1 shows the expected changes in W_{Trsp}, W_{Force}, Av$[Ca^{2+}]_c$, and NADH for each protocol.

Method 2. The first-order derivatives were calculated from Eq. 3 (with $\phi = 0$ as above) according to

$$\frac{\mathrm{d(NADH\ MIN)}}{\mathrm{d(Freq)}} = \beta + 2 \cdot \gamma \cdot \mathrm{Freq}, \tag{4a}$$

$$\frac{\mathrm{d(NADH\ MIN)}}{\mathrm{d}(F_{Av})} = \delta + 2 \cdot \epsilon \cdot F_{Av}, \tag{4b}$$

and were evaluated at reference point 7 in Fig. 3 *A*. To compare the derivatives for frequency versus F_{Av}, F_{Av} was normalized to unity (frequency was already at unity since the selected reference point was at 1 Hz). The pooled data ($N = 6$) from the surface analysis showed similar changes in NADH MIN with respect to frequency (W_{Trsp}; -0.118 ± 0.018) and F_{Av} (W_{Force}; -0.083 ± 0.019). Thus, the conclusion that increased W_{Force} or W_{Trsp} stimulate oxidative phosphorylation similarly was confirmed by this second analysis method.

W_{Force} and W_{Trsp} cross-interaction. To investigate the possibility of a cross-interaction, the interactive term ($\phi \cdot \mathrm{Freq} \cdot F_{Av}$) in Eq. 3 was included when fitting the NADH MIN data. Using an *F* test (see "Methods"), it was found that, in five out of the six trabeculae, the extra term did not cause a significantly better fit of the data. The data was nevertheless fit while including the interactive term, and its relevance evaluated by repeating the surface analysis above and comparing the results when using the two different common reference points; 0 versus 7 (Fig. 3 *A*). F_{Av} was thus doubled ($F^0_{Av}/2$ to F^0_{Av}) at either 2 Hz (0–3) or 1 Hz (4–7) and frequency was doubled (1 to 2 Hz) at either F^0_{Av} (0–4) or $F^0_{Av}/2$ (3–7). That is, W_{Force} was increased at two different W_{Trsp}, and W_{Trs} was increased at two different W_{Force}. Using either common reference point, each resulted in a similar fall of NADH when work was increased either by increased W_{Force} or by W_{Trsp}. Based on these results, we find no evidence for a dependency between W_{Force} and W_{Trsp}.

Comparing the Effects of W_{Force} versus Av$[Ca^{2+}]_c$ on NADH REC and NADH MAX

The second goal of this study is to determine if the NADH recovery, which depends on Av$[Ca^{2+}]_c$ [as we have shown previously (Brandes and Bers, 1997)], also depends on W_{Force} by possibly altering the Ca^{2+}-sensitivity ($K_{0.5}$) of the mitochondrial dehydrogenases. Figure 5 *A* shows the effects of increased frequency and SL (and consequently F_{Av}) on NADH REC. The spheres are the NADH REC data points

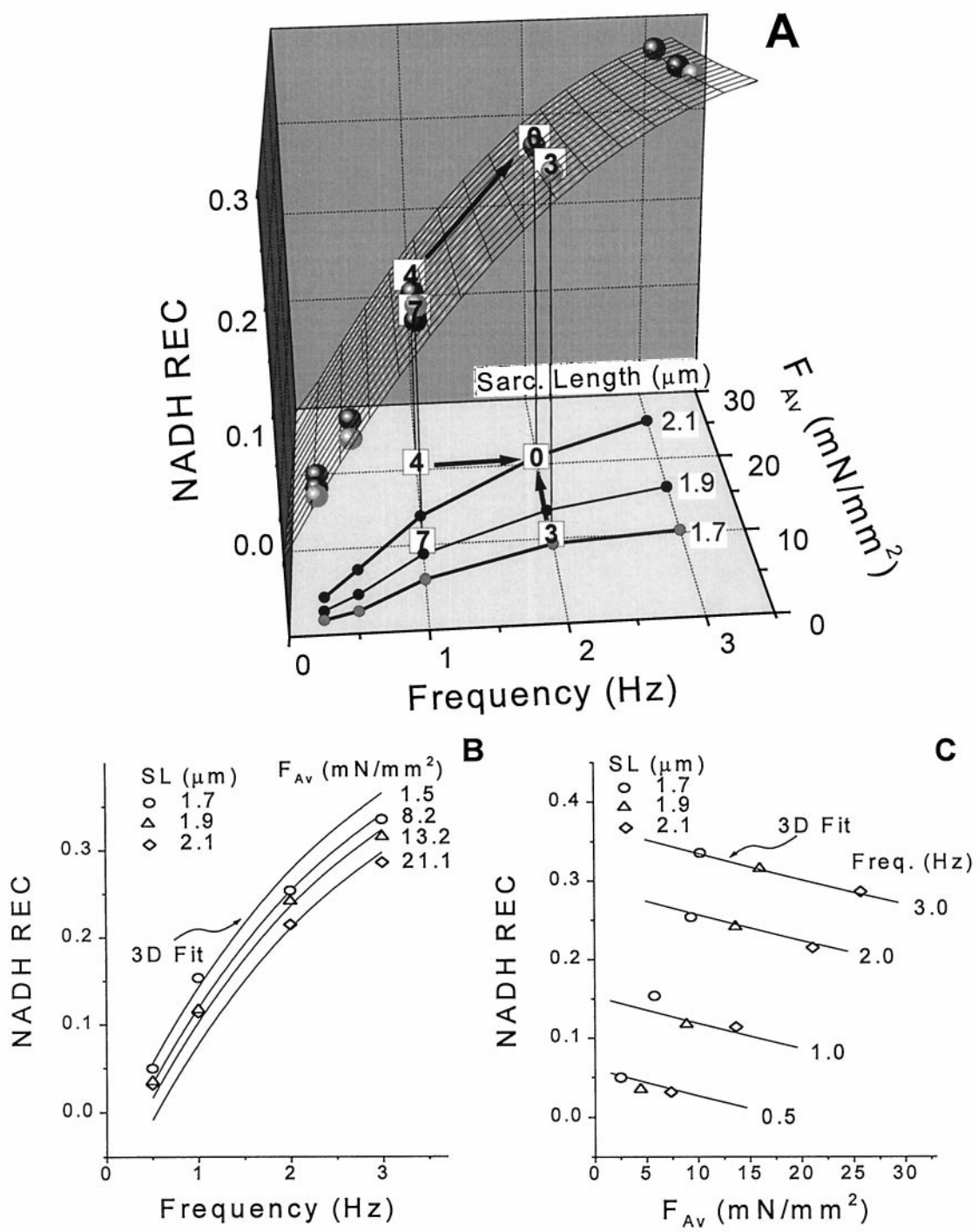

FIGURE 5 A typical example of the relationship between NADH REC (z axis) versus pacing frequency (x axis) and calculated F_{Av} (y axis). *A*. The spheres are the NADH REC data points, obtained at the indicated frequency and SL (producing the calculated F_{Av} on the y axis). The wire-frame surface was calculated using a multiple linear regression fit (see Eq. 3). The numbers in squares (at Reference and comparison points) are calculated NADH REC values at various frequencies and F_{Av}s (see Table 1). *B*. NADH REC versus frequency along lines of constant F_{Av}, calculated from the fitted surface parameters. *C*. NADH REC versus F_{Av} along lines of constant frequency (Freq.), calculated from the fitted surface parameters. Relevant data points at various sarcomere lengths are also shown in *B* and *C*.

whereas the wire frame surface was calculated using Eq. 3 as previously.

Figure 5 *B* shows NADH REC calculated at various constant F_{Av}s (*solid lines*) using the parameters obtained from the fitted surface in Fig. 5 *A*, together with some of the experimental data points. Figure 5 *B* demonstrates that, at constant F_{Av} (and therefore constant W_{Force}), increased frequency, and therefore increased Av$[Ca^{2+}]_c$ (and W_{Trsp}), results in enhanced NADH recovery, presumably due to stimulation of the NADH production rate. Figure 5 *B* also

shows that the relationship between NADH REC and frequency is relatively insensitive to F_{Av}; increasing F_{Av} up to 14 times only caused a small downward shift of the NADH REC versus the frequency curve. This is further illustrated in Fig. 5 *C*.

Figure 5 *C* shows NADH REC calculated at various constant frequencies (*solid lines*) using the parameters obtained from the fitted surface in Fig. 5 *A*, together with the experimental data points. Figure 5 *C* demonstrates that increased W_{Force} by itself (at constant $Av[Ca^{2+}]_c$ due to constant frequency) does not cause large changes in NADH REC. A simple comparison based on Fig. 5, *B* and *C*, shows that a sixfold increase in frequency or $Av[Ca^{2+}]_c$, at constant W_{Force}, increased NADH REC by ~0.30 units (Fig. 5 *B*). Similarly, a sixfold increase in F_{Av} (increased W_{Force}), at constant frequency (and $Av[Ca^{2+}]_c$), produced a comparably small decrease of NADH REC by ~0.07 units (Fig. 5 *C*). Fig. 5, *B* and *C* combined, suggest that increased $Av[Ca^{2+}]_c$, rather than W_{Force}, is the major factor contributing to increased NADH REC when the pacing frequency is increased.

To quantify the sensitivity of NADH REC to increased W_{Force} versus increased $Av[Ca^{2+}]_c$, the properties of the fitted surface in Fig. 5 *A* were evaluated in a manner analogous to the evaluation of Fig. 3 *A*. Figure 4 *A* shows pooled data ($N = 6$) of the magnitude of NADH REC in Fig. 5 *A*, using the same reference and comparison points as defined in Fig. 3 *A*. Figure 4 *B* shows the difference between the reference and comparison points, together with the previous results from the analysis of the data in Fig. 2, *B* and *C*, where work was increased by increasing both W_{Trsp} and W_{Force}.

Figure 4 *B* demonstrates that, when only W_{Force} was increased (by doubling $F^0_{Av}/2$ by increasing SL, P0–3), NADH REC was unchanged, 1.0 ± 1.7% (not significant). In contrast, when only $Av[Ca^{2+}]_c$ (and W_{Trsp}) were increased [by doubling frequency (1 to 2 Hz) and reducing SL, P0–4], NADH REC was 10.0 ± 1.9% larger. Consequently, when both $Av[Ca^{2+}]_c$ and W_{Force} were increased, NADH REC was still only 10.1 ± 1.15% larger [by doubling frequency (1 to 2 Hz at constant SL), resulting in F_{Av} increasing by a factor of 1.53, P0–1]. This indicates that any contribution from W_{Force} was negligible, and the recovery solely depends on $Av[Ca^{2+}]_c$. Indeed, when frequency was more than doubled (by increasing frequency from ~0.7 to 2 Hz at constant SL so that $F^0_{Av}/2$ doubled, P0–2), NADH REC was 15.8 ± 1.8% larger. Thus, only $Av[Ca^{2+}]_c$ significantly contributes as a factor in stimulating NADH recovery during sustained work, presumably by slowly increasing the $[Ca^{2+}]_m$.

The curvature of the NADH REC surfaces were also calculated (as for NADH MIN), and were found to be 0.139 ± 0.018 and −0.004 ± 0.012 along frequency ($Av[Ca^{2+}]_c$) and F_{Av} (W_{Force}), respectively. Thus, also this second analysis method showed that only $Av[Ca^{2+}]_c$ is important for NADH recovery.

NADH MAX was finally analyzed ($N = 6$) in analogy with the NADH REC data. Figure 4 *B* shows that, when only W_{Force} was increased (by doubling $F^0_{Av}/2$ by increasing SL, P0–3), NADH MAX was unchanged 1.4 ± 1.7% (not significant), but that, when only $Av[Ca^{2+}]_c$ was increased, (by doubling frequency and reducing SL, P0–4), NADH MAX was 7.5 ± 1.5% larger. Furthermore, when both $Av[Ca^{2+}]_c$ and W_{Force} were increased, NADH MAX was still 7.24 ± 1.63% larger (by doubling frequency, resulting in F_{Av} increasing by a factor of 1.53, P0–1) or 12.1 ± 1.0% larger (by increasing frequency so that $F^0_{Av}/2$ doubled, P0–2). These results are, as expected, similar to the result from the analysis of NADH REC.

Effects of $[Ca^{2+}]_o$ (and frequency) on $[NADH]_m$ regulation

Increased SL leads to increased F_{Av} and W_{Force} without significantly altering $Av[Ca^{2+}]_c$. In contrast, elevation of $[Ca^{2+}]_o$ is expected to increase both W_{Force} and $Av[Ca^{2+}]_c$ (and consequently W_{Trsp}). Increased $[Ca^{2+}]_o$ is thus similar to increased frequency. However, increased frequency produces only small changes of the Ca^{2+}-transient amplitude, whereas increased $[Ca^{2+}]_o$ produces a larger Ca^{2+}-transient amplitude at the same frequency. The two protocols, increased frequency versus increased $[Ca^{2+}]_o$, may therefore affect W_{Trsp} and $[Ca^{2+}]_m$-uptake differently and could, consequently, have differing impact on $[NADH]_m$ regulation.

Figure 6 *A* shows an example of the NADH response to increasing frequency at $[Ca^{2+}]_o = 0.3$ and 2 mM. At both concentrations, increasing frequency caused progressively lower NADH MIN but larger NADH REC and NADH MAX, as was also shown in Fig. 2 *A*. At $[Ca^{2+}]_o = 0.3$ mM, however, the deviations from baseline were much smaller than at 2 mM.

Similar to the previous group of trabeculae (where the effects of changes in SL were studied), doubling the frequency from 1 to 2 Hz caused F_{Av} to increase by a factor of 1.48 ± 0.06 (at a time corresponding to NADH MIN; $N = 4$; no significant difference between the two groups).

$[NADH]_m$ *versus frequency.* Figure 6 *B* shows NADH MIN, NADH REC, and NADH MAX versus frequency at $[Ca^{2+}]_o = 0.3$ and 2 mM (data obtained from the example in Fig. 6 *A*). At a constant frequency, the higher $[Ca^{2+}]_o$ results in a larger fall of NADH (lower MIN) and also larger NADH REC and NADH MAX. This effect of $[Ca^{2+}]_o$ is more pronounced at higher frequencies. Because increased $[Ca^{2+}]_o$ is associated with higher $Av[Ca^{2+}]_c$, W_{Trsp}, and, consequently, higher F_{Av}, the lower MIN may be due to higher W_{Trsp} and W_{Force}, whereas the higher REC and MAX may be due to higher $Av[Ca^{2+}]_c$. The sensitivity of NADH to increased frequency was again calculated as was done for the previous group of trabeculae (where SL was varied; Table 1, P0–1), and similar results were obtained: when the frequency was increased to 2 rather than to 1 Hz at SL = 2.1 μm and $[Ca^{2+}]_o = 2.0$ mM, NADH MIN was 0.107 ±

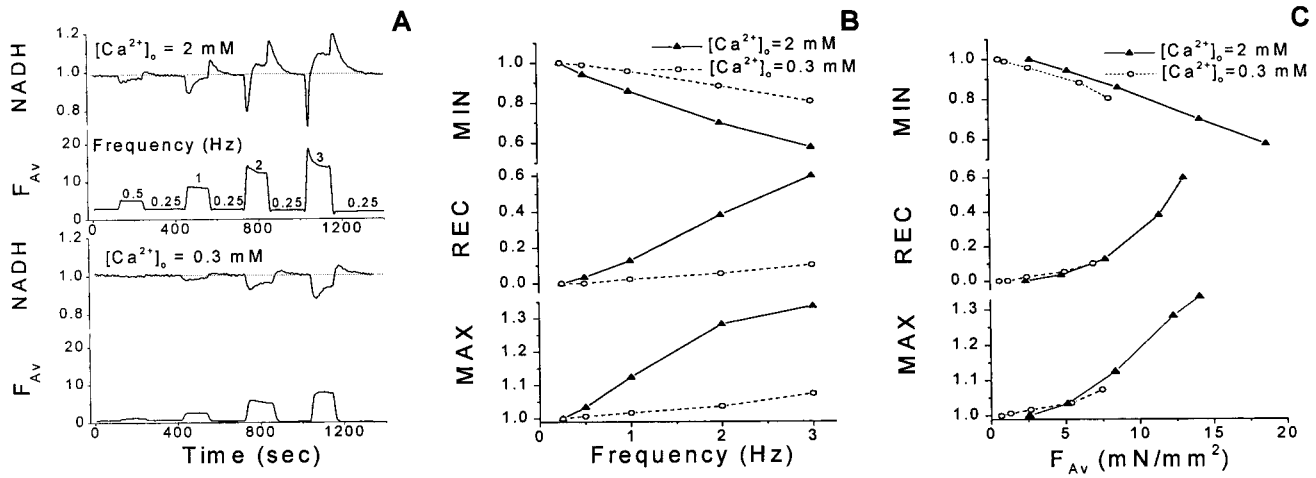

FIGURE 6 A typical example of the effect of increased pacing frequency (increased work and Av$[Ca^{2+}]_c$) and increased $[Ca^{2+}]_o$ (increased work and Av$[Ca^{2+}]_c$) on $[NADH]_m$. *A*. Time-traces of average force (F_{Av}; mN/mm^2) and NADH (relative to 0.25 Hz) as frequency was increased from control of 0.25 Hz to 0.5, 1, 2, or 3 Hz, and then back to 0.25 Hz at $[Ca^{2+}]_o$ = 0.3 and 2 mM. *B*. NADH MIN, NADH REC, and NADH MAX as a function of pacing frequency and $[Ca^{2+}]_o$. *C*. NADH MIN, NADH REC, and NADH MAX as a function of F_{Av} and $[Ca^{2+}]_o$. F_{Av} was obtained at each pacing frequency (0.25, 0.5, 1, 2, and 3 Hz) from Fig. 6 *A*.

0.020 units lower, NADH REC was 0.134 ± 0.040 units larger and NADH MAX was 0.111 ± 0.018 units larger (N = 4).

$[NADH]_m$ *versus* F_{Av}. Figure 6 *C* shows NADH MIN, NADH REC, and NADH MAX versus F_{Av} at $[Ca^{2+}]_o$ = 0.3 and 2 mM (data obtained from the example in Fig. 6 *A*). To compare $[Ca^{2+}]_o$ = 0.3 with 2 mM at the same F_{Av}, it is necessary to alter the pacing frequency. Thus, although the two concentrations can be compared at the same W_{Force} using this approach, W_{Trsp}, and therefore total Work, may be different. At $[Ca^{2+}]_o$ = 0.3 versus 2 mM and constant F_{Av} (but higher frequency), MIN is only slightly lower and REC and MAX are relatively unchanged. The similar MIN may be explained by similar W_{Trsp}, and the unchanged REC and MAX is consistent with constant Av$[Ca^{2+}]_c$ (reflected in constant F_{Av}). This would suggest that the resulting Av$[Ca^{2+}]_c$ is the dominant factor in determining W_{Trsp} and $[Ca^{2+}]_m$-uptake, with little or no differential effects of frequency versus Ca^{2+}-transient amplitude.

To determine the effects of doubling F_{Av} on NADH MIN, NADH MAX, and NADH REC, as was also done for the previous group of trabeculae (where SL was varied), the data in Fig. 6 *C* were fit to second-degree polynomials and analyzed analogously (N = 4). From this analysis, it was found that, when $F^0_{Av}/2$ was doubled by increased frequency (~0.7 to 2 Hz) at $[Ca^{2+}]_o$ = 2 mM and SL = 2.1 μm (Table 1, P0–2), NADH MIN was lower by 16.6 ± 1.9%, NADH REC was higher by 21.7 ± 4.8%, and NADH MAX was higher by 18.2 ± 1.0%. These results were again similar to the previous group of trabeculae.

3D analysis of NADH MIN, NADH REC, and NADH MAX

Figure 7 *A* shows results from 3D analysis (N = 4) of the $[Ca^{2+}]_o$-frequency data (analogous to the results in Fig. 4 *A*, which were obtained from analysis of the SL–frequency data). The usual Reference (P0) was used to obtain the absolute values of NADH MIN-1, NADH REC, and NADH MAX-1, but different comparison protocols were used here (versus those used in Figs. 3 *A* and 5 *A*). In this case, P5 produced $F^0_{Av}/2$ due to lower $[Ca^{2+}]_o$, (at the same frequency as the Reference) and P6 keeps F_{Av} constant (at F^0_{Av}) while increasing $[Ca^{2+}]_o$ and lowering the frequency. Figure 7 *B* shows the calculated ΔNADH by comparing P0 versus P5 (P0–5) and P0 versus P6 (P0–6). The results from the analysis of the data in Fig. 6, *B* and *C*, where work was increased by increasing frequency at constant $[Ca^{2+}]_o$, and thus increasing both W_{Trsp} and W_{Force}, are also shown for comparison.

Figure 7 *B* shows that, when $F^0_{Av}/2$ was doubled by increased $[Ca^{2+}]_o$ (P0–5), NADH MIN was 14.3 ± 1.6% lower. This difference is similar to the lower NADH MIN observed when $F^0_{Av}/2$ was doubled by increased pacing frequency (P0–2; ΔNADH MIN = −16.6 ± 1.9%). In both cases, it is expected that the increased Av$[Ca^{2+}]_c$ results in increased W_{Trsp} and W_{Force}. In contrast, the difference is larger than when $F^0_{Av}/2$ was doubled by increased SL (Fig. 4 *B*, P0–3; only increased W_{Force}; ΔNADH MIN = −8.0 ± 2.0%) or when frequency was doubled at constant F_{Av} (Fig. 4 *B*, P0–4; only increased W_{Trsp}; ΔNADH MIN = −9.2 ± 1.1%). These results are consistent with the idea that, by increasing either frequency or $[Ca^{2+}]_o$, both W_{Force} and W_{Trsp} increased, causing a ΔNADH MIN that was comparable to the sum of the separate ΔNADH MINs for increased W_{Force} and W_{Trsp}.

Comparing Ca^{2+}-amplitude versus frequency on W_{Trsp}. The first part of our third goal is to determine if W_{Trsp}, contributing to the initial fall of NADH, depends on frequency versus Ca^{2+}-transient amplitude ($[Ca^{2+}]_o$). Figure 7 *B* shows that the fall of NADH MIN was similar when

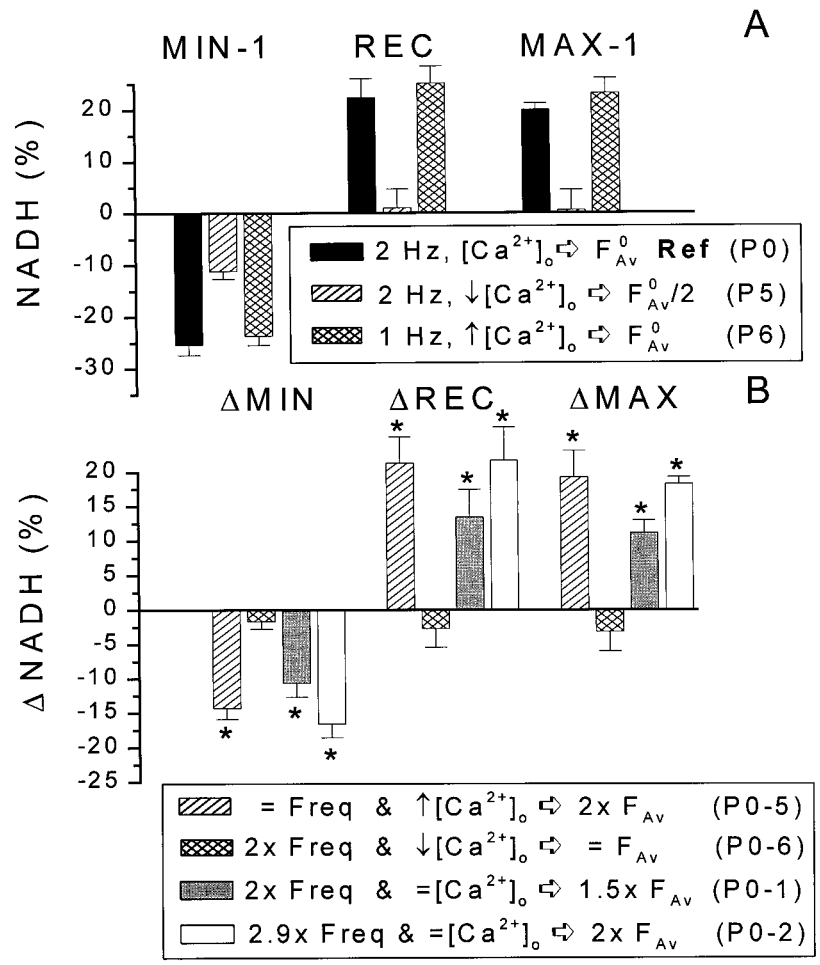

FIGURE 7 Pooled data from fitted wire frame surfaces similar to Figs. 3 *A* and 5 *A* except that $[Ca^{2+}]_o$, rather than SL, was varied. *A*. Values for NADH MIN-1, NADH REC, and NADH MAX-1 using Reference protocol P0 and two comparison protocols, P5 and P6 (see Table 1). *B*. Differences in NADH; ΔMIN, ΔREC, and ΔMAX obtained by subtracting calculated NADH values, obtained from P5 and P6, from P0 (Table 1); P0–5 (*hatched*; at constant frequency (Freq. = 2 Hz), increase $[Ca^{2+}]_o$ to double F_{Av} ($F^0_{Av}/2$ to F^0_{Av}) and P0–6 (*cross-hatched*; double frequency (1 to 2 Hz) and decrease $[Ca^{2+}]_o$ to obtain constant F_{Av} (F^0_{Av})). Also shown are the changes calculated from Fig. 6 according to P0–1 (*gray*); double frequency (1 to 2 Hz at constant SL) to increase F_{Av} 1.5 times ($F^0_{Av}/1.5$ to F^0_{Av}) and P0–2 (*white*); increase frequency 2.9 times (~0.7 to 2 Hz at constant SL) to double F_{Av} ($F^0_{Av}/2$ to F^0_{Av}). The * indicates that a difference is significantly larger than zero. Table 1 shows expected changes in W_{Trsp}, W_{Force}, $Av[Ca^{2+}]_c$, and NADH for each protocol.

$F^0_{Av}/2$ was doubled by increased $[Ca^{2+}]_o$ (P0–5) as when $F^0_{Av}/2$ was doubled by increased frequency (P0–2) (ΔNADH MIN = −16.6 ± 1.9% versus −14.3 ± 1.6%). Because $F^0_{Av}/2$ increased by the same amount in both cases, it may be assumed that $Av[Ca^{2+}]_c$ also increased by similar amounts (Brandes and Bers, 1997). This result would argue against any differential effects of frequency versus Ca^{2+}-transient amplitude on W_{Trsp}.

An alternative way to evaluate, in a single protocol, how the initial fall of NADH, which is partly due to W_{Trsp}, depends on frequency versus Ca^{2+}-transient amplitude is to double the frequency and to lower $[Ca^{2+}]_o$ to keep F_{Av} constant (P0–6). Figure 7 *B* shows that NADH MIN did not change significantly (−1.7 ± 1.0%). Because W_{Force} was kept constant and NADH MIN did not change, W_{Trsp} must therefore also not have changed significantly. Thus, both results above suggest that the work needed to transport Ca^{2+} (W_{Trsp}) may be similar when using low frequency combined with high Ca^{2+}-transient amplitude as when using high frequency combined with low Ca^{2+}-transient amplitude (provided that $Av[Ca^{2+}]_c$ is the same in both cases).

Comparing Ca^{2+}–amplitude versus frequency on $[Ca^{2+}]_m$-uptake. The second part of our third goal is to determine if the $[Ca^{2+}]_m$-uptake, controlling NADH REC, depends on frequency versus Ca^{2+}-transient amplitude at the same $Av[Ca^{2+}]_c$. Figure 7 *B* shows that ΔNADH REC was similar when $F^0_{Av}/2$ was doubled by increased $[Ca^{2+}]_o$ (P0–5) as when $F^0_{Av}/2$ was doubled by increased frequency (P0–2) (ΔNADH REC = 21.3 ± 3.8% versus 21.7 ± 4.8%). Figure 7 *B* also shows that NADH REC did not change significantly (ΔNADH REC = −2.7 ± 2.7%) when the frequency was doubled (1 to 2 Hz) and $[Ca^{2+}]_o$ lowered to keep F_{Av} (and therefore, presumably, $Av[Ca^{2+}]_c$) constant (P0–6). As expected, the results for NADH MAX were similar to the results obtained for NADH REC.

These results suggest that NADH REC (and NADH MAX) are similar for a particular $Av[Ca^{2+}]_c$, regardless of whether low frequency is combined with high Ca^{2+}-transient amplitude or if high frequency is combined with low Ca^{2+}-transient amplitude to obtain a particular $Av[Ca^{2+}]_c$. The similar NADH REC (and NADH MAX) would therefore suggest that the $[Ca^{2+}]_m$-uptake is similar in both cases.

Effects of temperature (and frequency) on $[NADH]_m$ regulation

The fourth goal is to determine if the mechanisms responsible for the smaller under- and overshoot at elevated temperatures are consistent with lower $Av[Ca^{2+}]_c$. Figure 8 *A* shows an example of the NADH response to increasing

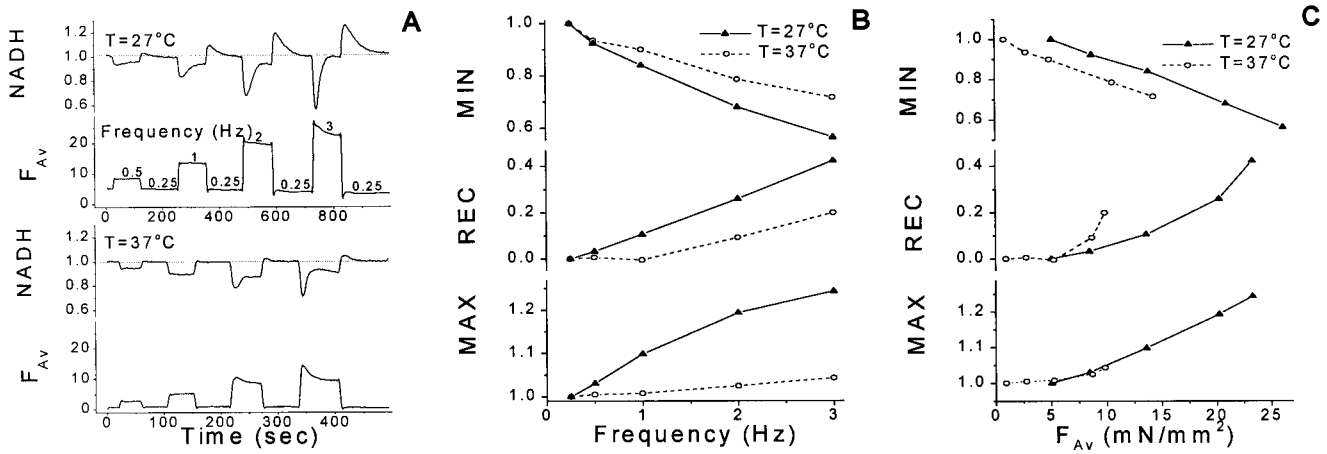

FIGURE 8 A typical example of the effect of increased pacing frequency (increased work and Av$[Ca^{2+}]_c$) and increased temperature (decreased work and Av$[Ca^{2+}]_c$) on $[NADH]_m$. *A*. Time-traces of average force (F_{Av}; mN/mm^2) and NADH (relative to 0.25 Hz) as frequency was increased from control of 0.25 Hz to 0.5, 1, 2, or 3 Hz, and then back to 0.25 Hz at 27°C and 37°C. *B*. NADH MIN, NADH REC, and NADH MAX as a function of pacing frequency and temperature. *C*. NADH MIN, NADH REC, and NADH MAX as a function of F_{Av} and temperature. F_{Av} was obtained at each pacing frequency (0.25, 0.5, 1, 2, and 3 Hz) from Fig. 8 *A*. (Notice qualitative similarity with Fig. 6).

frequency at 27 and 37°C. At both temperatures, increasing frequency caused progressively lower NADH MIN but larger NADH REC and NADH MAX, as was also shown in Figs. 2 *A* and 6 *A*. At 37°C, however, the deviations from baseline were much smaller, and the pacing frequency had to be increased up to ~6 Hz at 37°C to obtain similar deflections to those at 3 Hz and 27°C (not shown) (Brandes and Bers, 1997).

$[NADH]_m$ versus Frequency. Figure 8 *B* shows *NADH* MIN, NADH REC, and NADH MAX versus frequency at 27°C and 37°C (data obtained from the example in Fig. 8 *A*). At a constant frequency, the lower temperature results in a larger fall of NADH (lower MIN) and also larger REC and MAX. This effect of temperature is more pronounced at higher frequencies. Because decreased temperature is associated with higher Av$[Ca^{2+}]_c$, and consequently higher F_{Av}, W_{Force}, and W_{Trsp}, the lower MIN may be due to higher W_{Trsp} and W_{Force}, whereas the higher NADH REC and NADH MAX may be due to higher Av$[Ca^{2+}]_c$. To further test this hypothesis, the effect of temperature on $[NADH]_m$ at a fixed F_{Av} (rather than frequency) was calculated.

$[NADH]_m$ versus F_{Av}. Figure 8 *C* shows NADH MIN, NADH REC, and NADH MAX versus F_{Av} at 27°C and 37°C (data obtained from the example in Fig. 8 *A*). To compare the two temperatures at the same F_{Av}, it is necessary to increase the pacing frequency. Thus, although the two temperatures can be compared at the same W_{Force} using this approach, W_{Trsp}, and therefore total work, may be different. At 37°C versus 27°C and constant F_{Av} (but higher frequency), *NADH* MIN is slightly lower but NADH REC and NADH MAX are relatively unchanged. A slightly larger W_{Trsp} may explain the slightly lower NADH MIN, and a constant Av$[Ca^{2+}]_c$ (reflected in constant F_{Av}), with no significant effect of frequency versus Ca^{2+}-transient amplitude, may explain the unchanged NADH REC and NADH MAX.

Figures 6 and 8 show a similar dependence of NADH on frequency and F_{Av}, regardless of whether F_{Av} (and therefore, presumably, Av$[Ca^{2+}]_c$) was controlled by $[Ca^{2+}]_o$ or temperature. This is consistent with the idea that, at least partially, the effects of temperature on the modulation of the relationship between $[NADH]_m$ and frequency is caused by the effect of temperature on Av$[Ca^{2+}]_c$.

3D analysis of NADH MIN, NADH REC, and NADH MAX

A 3D analysis was also performed on the temperature data, and the results (not shown) were similar to those for the $[Ca^{2+}]_o$ data (Fig. 7). (The slightly lower NADH MIN at 37°C and constant F_{Av}, was not significant). These results are again consistent with the idea that the lower under- and overshoot observed at higher temperatures are, at least partially, due to the effect of temperature in lowering Av$[Ca^{2+}]_c$.

DISCUSSION

The main findings of this study are:

1. The initial fall of NADH during increased pacing frequency depends independently on increased myofilament work and on increased Ca^{2+}- transport ATPase activity.
2. The NADH recovery process depends on Av$[Ca^{2+}]_c$, but not on absolute work level, suggesting that the Ca^{2+}-sensitivity of the mitochondrial dehydrogenases is independent of work level.
3. The initial NADH fall, due to work by Ca^{2+}-transport activity (W_{Trsp}), and the NADH recovery are similar whether caused by low frequency and high Ca^{2+}-transient amplitude or vice versa (provided that W_{Force} and Av$[Ca^{2+}]_c$ is similar in both cases). This suggests that

both W_{Trsp} and the $[Ca^{2+}]_m$-uptake depend mainly on $Av[Ca^{2+}]_c$ rather than on a differential influence of amplitude versus frequency.

4. The mechanisms associated with the lower under- and overshoot, observed at elevated temperature (37°C), may be explained by lowered $Av[Ca^{2+}]_c$ and myofilament work. The NADH control mechanisms that operate at lower temperatures are thus qualitatively similar at higher, more physiological temperatures.

Effects of sarcomere length (and frequency) on $[NADH]_m$ regulation

We have previously demonstrated that increased work initially caused a rapid fall of $[NADH]_m$ (Brandes and Bers, 1996a; Brandes and Bers, 1997). This fall occurred both when increased work was caused by increased $Av[Ca^{2+}]_c$ (increased pacing frequency or $[Ca^{2+}]_o$) or during constant $Av[Ca^{2+}]_c$ (by increased sarcomere length). Those results, therefore, suggested that work by itself resulted in a control signal (e.g., increased [ADP] (From et al., 1990)) that stimulated an increased rate of oxidative phosphorylation, and thereby the fall of $[NADH]_m$. What was unclear, however, was to what extent this control signal was generated as a consequence of myofilament work versus other nonforce-generating work (e.g., Ca^{2+}-transport). Thus, the isolated effects of myofilament versus Ca^{2+}-transport work (W_{Force} versus W_{Trsp}) on NADH MIN were determined.

Comparing the effects of W_{Force} versus W_{Trsp} on NADH MIN

Figure 4 *B* shows that both increased W_{Force} and W_{Trsp} caused a similar fall of $[NADH]_m$, suggesting that each type of work caused a similar stimulation of the oxidative phosphorylation rate. This stimulation, in turn, is expected to depend on the amount of control signal being generated (e.g., [ADP]) and on the coupling between the signal source, myofilaments or SR, to the mitochondria. It is generally believed that a larger fraction of ATP is being hydrolyzed by the myofilaments than by the SR Ca^{2+}-ATPase (or other nonforce-generating processes) during each contraction cycle (Ebus and Stienen, 1996). If this is the case, the amount of control signal generated from the W_{Trsp} process may be lower than that from W_{Force}. Consequently, to produce similar declines of $[NADH]_m$, the coupling between the SR and the mitochondria, therefore, appears to be stronger than the coupling between the myofilaments and the mitochondria. A close coupling between the SR and mitochondria are consistent with recent work showing a cross-talk between the SR and mitochondrial Ca^{2+} in rat myocytes (Sharma et al., 1998).

A second explanation for the relatively large effect of increased W_{Trsp} on NADH MIN is that it may be a smaller increase of ATP hydrolysis rate when doubling $F^0_{Av}/2$ at constant W_{Trsp} (by increasing SL) versus doubling frequency at constant W_{Force} (by simultaneously reducing SL). This could imply that the efficiency of contraction may be lower (i.e., more ATP/F_{Av} consumed) at shorter sarcomere lengths. However, previous studies have shown a linear relationship between ATP consumption rate and sarcomere length (Kentish and Stienen, 1994), making this explanation unlikely.

A third explanation for the apparent large effect of increased W_{Trsp} on NADH MIN is that it may be due to increased NADH consumption by stimulation of the mitochondrial F_oF_1 ATP-synthase during increased $[Ca^{2+}]_c$ (Doumen et al., 1995) (because only increased W_{Trsp} but not W_{Force} is associated with increased $[Ca^{2+}]_c$). Although we have previously shown that increased $[Ca^{2+}]_c$ was not needed to initially stimulate the oxidative phosphorylation rate (and, consequently, the fall of $[NADH]_m$) (Brandes and Bers, 1997), it is possible that increased $[Ca^{2+}]_c$ may act as a supplementary control signal.

Comparing the effects of W_{Force} versus $Av[Ca^{2+}]_c$ on NADH REC and NADH MAX

The NADH production rate, and consequently NADH recovery, may be stimulated by increased [ADP]/[ATP] by increasing the Ca^{2+}-sensitivity of mitochondrial dehydrogenases (McCormack et al., 1990). We, therefore, investigated the effects of increased W_{Force} on the Ca^{2+}-dependent NADH recovery. Figure 4 *B* confirms our previous results (Brandes and Bers, 1997), demonstrating increased NADH REC for increased frequency and $Av[Ca^{2+}]_c$. Figure 4 *B* additionally demonstrates that increased W_{Force} did not enhance this slow NADH recovery, suggesting that [ADP]/[ATP] does either not increase, or does not influence the Ca^{2+}-dependent stimulation of the NADH production rate during the recovery phase. The absence of increased recovery with increased W_{Force} also suggests that the increase in SL (which was used to increase W_{Force}) did not cause large changes in $Av[Ca^{2+}]_c$ (Kentish and Wrzosek, 1998).

Larger $[Ca^{2+}]_m$ is expected after increased work by increased frequency or $[Ca^{2+}]_o$, thus producing a larger $[NADH]_m$ overshoot (NADH MAX) when work is reduced to control (Fig. 4 *B*). As for NADH REC, increased W_{Force} did not cause increased NADH MAX, suggesting that any alterations in [ADP]/[ATP] is also not important in stimulating the NADH production rate during the overshoot phase.

Effects of $[Ca^{2+}]_o$ (and frequency) on $[NADH]_m$ regulation

Both increased pacing frequency and increased Ca^{2+}-transient amplitude increase work and $Av[Ca^{2+}]_c$ (Brandes and Bers, 1997). The effect of these two protocols on W_{Trsp} and, consequently, the initial fall of $[NADH]_m$ and the $[NADH]_m$ recovery may be directly compared provided that F_{Av} and $Av[Ca^{2+}]_c$ are identical in both cases. $Av[Ca^{2+}]_c$ was not measured directly here, but, because F_{Av} is proportional to $Av[Ca^{2+}]_c$ (Maier et al., 1998; Brandes et al., 1998), it was

assumed that changes in F_{Av} reflect proportional changes in $Av[Ca^{2+}]_c$.

Figure 7 *B* shows that when $F^0_{Av}/2$ is doubled by increasing either the frequency or Ca^{2+}-transient amplitude (by increasing $[Ca^{2+}]_o$), the changes in NADH MIN, NADH REC, and NADH MAX are similar. Furthermore, when the frequency is increased and $[Ca^{2+}]_o$ lowered to keep F_{Av} (and, presumably, $Av[Ca^{2+}]_c$) constant, there are no significant differences in NADH MIN, NADH REC, or NADH MAX. Because there were no changes in NADH MIN, the increase in the ATP consumption rate (causing the fall of $[NADH]_m$) therefore appears to be similar, regardless of whether work (W_{Trsp}) is increased by increased frequency or Ca^{2+}-transient amplitude. Furthermore, because there were no changes in NADH REC or NADH MAX, this suggests that at constant $Av[Ca^{2+}]_c$, the $[Ca^{2+}]_m$-uptake is similar regardless of whether $Av[Ca^{2+}]_c$ is increased by increased frequency or Ca^{2+}-transient amplitude.

These results are somewhat different from our earlier preliminary results showing that $[NADH]_m$, at steady state, was higher when F_{Av} was similarly increased by increased $[Ca^{2+}]_o$ versus frequency (Brandes and Bers, 1996b). However, our methods in that report were specifically designed to answer the question of the effects of frequency versus increased Ca^{2+}-transient amplitude on $[NADH]_m$ at steady state (rather than the acute regulatory phases). It is likely that the methods used in this current work were not sensitive enough to determine a significant difference in recovery, and we also did not determine $[NADH]_m$ at steady state here. Other investigators have also proposed and shown that, in isolated mitochondria, a Ruthenium Red-insensitive rapid uptake mode may depend on both Ca^{2+} pulse shape and frequency (Sparagna et al., 1995). Further studies are clearly required to determine if this rapid uptake mode is also present in intact trabeculae, and whether the $[Ca^{2+}]_m$ uptake only depends on $Av[Ca^{2+}]_c$ or also on Ca^{2+} pulse shape and frequency.

Effects of temperature (and frequency) on $[NADH]_m$ regulation

Comparable frequency steps at 37°C cause smaller changes in NADH than at 24–25°C (Fig. 8 and Brandes and Bers, 1997).

One explanation for this may be that it is due to altered kinetics such that, at 37°C, the up- and down-regulation of the NADH production rate may be relatively faster than the rise and fall of the NADH consumption rates. Consequently, during increased work, $[NADH]_m$ would start to recover earlier at 37°C than at 27°C, causing a smaller fall of NADH (higher NADH MIN). Conversely, when work is reduced, NADH would not accumulate to the same degree at 37°C as at 27°C, causing a smaller overshoot (lower NADH MAX). To test for temperature effects on the kinetics, we attempted to analyze the time constants for the NADH fall and recovery (not shown). It was, however, not possible to obtain unique estimates of relative changes, fall versus recovery time constants, at the two temperatures.

Another plausible explanation is the effect of temperature on $Av[Ca^{2+}]_c$ and consequently F_{Av}. Increased temperature causes reduced Ca^{2+}-transient amplitudes and faster relaxation rates (Puglisi et al., 1996), resulting in reduced $Av[Ca^{2+}]_c$ and, consequently, F_{Av}. Furthermore, within the temperature range studied here, the myofilament Ca^{2+}-sensitivity is relatively unaltered (Harrison and Bers, 1989). Comparison of Figs. 8 and 6 demonstrate that the effects of lowered temperature on NADH MIN, NADH REC, and NADH MAX (Fig. 8) were qualitatively similar to those of increased $[Ca^{2+}]_o$ (Fig. 6). This is consistent with the temperature effects on the $[NADH]_m$–frequency relationship being, at least partially, due to an effect of temperature on $Av[Ca^{2+}]_c$ (which was also confirmed by a 3D analysis). However, because temperature affects so many factors, interpretation of these experiments is necessarily more complex.

This work was supported by National Institutes of Health grants HL-57562 to R.B. and HL-52478 and HL-30077 to D.M.B.

REFERENCES

Ashruf, J. F., J. M. C. C. Coremans, H. A. Bruining, and C. Ince. 1995. Increase of cardiac work is associated with decrease of mitochondrial NADH. *Am. J. Physiol.* 269:H856–H862

Backx, P. H., and H. E. Ter Keurs. 1993. Fluorescent properties of rat cardiac trabeculae microinjected with fura-2 salt. *Am. J. Physiol.* 264: H1098–H1110.

Balaban, R. S. 1990. Regulation of oxidative phosphorylation in the mammalian cell. [Review]. *Am. J. Physiol.* 258:C377–C389.

Brandes, R., and D. M. Bers. 1996a. Increased work in cardiac trabeculae causes decreased mitochondrial NADH fluorescence followed by slow recovery. *Biophys. J.* 71:1024–1035.

Brandes, R., and D. M. Bers. 1996b. Stimulation of mitochondrial NADH production in cardiac trabeculae via protocols that raise cytosolic $[Ca^{2+}]$. *Biophys. J.* 70:A354 Abstract.

Brandes, R., and D. M. Bers. 1997. Intracellular Ca^{2+} increases the mitochondrial NADH concentration during elevated work in intact cardiac muscle. *Circ. Res.* 80:82–87.

Brandes, R., V. M. Figueredo, S. A. Camacho, and M. W. Weiner. 1994. Compensation for changes in tissue light absorption in fluorometry of hypoxic perfused rat hearts. *Am. J. Physiol.* 266:H2554–H2567.

Brandes, R., L. S. Maier, and D. M. Bers. 1998. Regulation of mitochondrial [NADH] by cytosolic $[Ca^{2+}]$ and work in trabeculae from hypertrophic and normal rat hearts. *Circ. Res.* 82:1189–1198.

Cooper, G., IV. 1979. Myocardial energetics during isometric twitch contractions of cat papillary muscle. *Am. J. Physiol.* 236:H244–H253.

Crompton, M. 1990. The role of Ca^{2+} in the function and dysfunction of heart mitochondria. *In* Calcium and the Heart. G. A. Langer, editor. Raven Press Ltd., New York. 167–199.

Doumen, C., B. Wan, and O. Ondrejickova. 1995. Effect of BDM, verapamil, and cardiac work on mitochondrial membrane potential in perfused rat hearts. *Am. J. Physiol.* 269:H515–H523.

Ebus, J. P., and G. J. Stienen. 1996. Origin of concurrent ATPase activities in skinned cardiac trabeculae from rat. *J. Physiol.* 492:675–687.

Eng, J., R. M. Lynch, and R. S. Balaban. 1989. Nicotinamide adenine dinucleotide fluorescence spectroscopy and imaging of isolated cardiac myocytes. *Biophys. J.* 55:621–630.

From, A. H., S. D. Zimmer, S. P. Michurski, P. Mohanakrishnan, V. K. Ulstad, W. J. Thoma, and K. Ugurbil. 1990. Regulation of the oxidative phosphorylation rate in the intact cell. *Biochemistry*. 29:3731–3743.

Hansford, R. G. 1991. Dehydrogenase activation by Ca^{2+} in cells and tissues. [Review]. *J. Bioenerg. Biomembr.* 23:823–854.

Hansford, R. G. 1994. Physiological role of mitochondrial Ca2+ transport. [Review]. *J. Bioenerg. Biomembr.* 26:495–508.

Harrison, S. M., and D. M. Bers. 1989. Influence of temperature on the calcium sensitivity of the myofilaments of skinned ventricular muscle from the rabbit. *J. Gen. Physiol.* 93:411–428.

Kentish, J. C., and G. J. Stienen. 1994. Differential effects of length on maximum force production and myofibrillar ATPase activity in rat skinned cardiac muscle. *J. Physiol.* 475:175–184.

Kentish, J. C., and A. Wrzosek. 1998. Changes in force and cytosolic Ca^{2+} concentration after length changes in isolated rat ventricular trabeculae. *J. Physiol.* 506:431–444.

Kobayashi, K., and J. R. Neely. 1983. Mechanism of pyruvate dehydrogenase activation by increased cardiac work. *J. Mol. Cell. Cardiol.* 15:369–382.

Maier, L. S., R. Brandes, B. Pieske, and D. M. Bers. 1998. Effects of Left ventricular hypertrophy on force and Ca^{2+} handling in isolated rat myocardium. *Am. J. Physiol. Heart Circulat. Physiol.* 43:H1361–H1370

McCormack, J. G., A. P. Halestrap, and R. M. Denton. 1990. Role of calcium ions in regulation of mammalian intramitochondrial metabolism. [Review]. *Physiol. Rev.* 70:391–425.

Nuutinen, E. M. 1984. Subcellular origin of the surface fluorescence of reduced nicotinamide nucleotides in the isolated perfused rat heart. *Basic Res. Cardiol.* 79:49–58.

Puglisi, J. L., R. A. Bassani, J. W. Bassani, J. N. Amin, and D. M. Bers. 1996. Temperature and relative contributions of Ca transport systems in cardiac myocyte relaxation. *Am. J. Physiol.* 270:H1772–H1778

Sharma, V. K., V. Ramesh, C. Franzini-Armstrong, and S. S. Sheu. 1998. Cross talk between sarcoplasmic reticular and mitochondrial Ca^{2+} in rat ventricular myocytes. *Biophys. J.* 74:A37–A37 Abstract.

Sparagna, G. C., K. K. Gunter, S. S. Shen, and T. E. Gunter. 1995. Mitochondrial calcium uptake from physiological-type pulses of calcium—A description of the rapid uptake mode. *J. Biol. Chem.* 270: 27510–27515.